Technical Support Document (TSD) for Adoption of the Generic Reaction Set Method (GRSM) as a Regulatory Non-Default Tier-3 NO2 Screening Option

EPA-454/R-24-005
November 2024

Technical Support Document (TSD) for Adoption of the Generic Reaction Set Method (GRSM) as a Regulatory Non-Default Tier-3 NO2 Screening Option

U.S. Environmental Protection Agency
Office of Air Quality Planning and Standards
Air Quality Assessment Division
Research Triangle Park, NC

Preface

This technical support document (TSD) provides a review of the Generic Reaction Set Method (GRSM) NO_2 option implementation and model performance in AERMOD version 23132. The purpose of this TSD is to support adoption of GRSM as a new regulatory non-default Tier 3 NO_2 screening option in AERMOD. The TSD presents and summarizes GRSM model performance based on four NO_2 model evaluation databases used to determine appropriate application of NO_2 screening options as part of the regulatory default version of AERMOD.

This version of the TSD revises the previous October 2023 version (EPA-454/R-23-005) to include supplemental performance and sensitivity modeling evaluations in a new Appendix A. These supplemental evaluations assess and compare refinements made to GRSM in AERMOD version 23132 that were not included in the GRSM code previously implemented in AERMOD version 22112. The refinements made to the GRSM code in AERMOD version 23132 include improvements to model behavior and performance owing to more realistic treatment of building effects on instantaneous plume spread and ozone entrainment, better accounting of multiple plume effects, and mitigating GRSM over-predictions in the far-field (e.g., beyond approximately 0.5 to 3 km for typical point source releases) while enhancing concentrations in the near-wake and far-wake building downwash zones (e.g., 10's to 100's of meters downwind) for some stack and building configurations.

All source code related to the formulation of the GRSM option in version 23132 has been preserved and is unchanged in version 24142. The requirement to include the BETA model option flag when using the GRSM option in version 23132 has been removed in version 24142.

Contents

Figures

Appendix Figures

Tables

1. Introduction

The proposed revisions to Appendix W to CFR 40 Part 51—*Guideline on Air Quality Models* (*Guideline*), includes a new version of AERMOD (23132)[1]. This new version of AERMOD includes a proposed regulatory non-default Tier 3 NO_2 screening option, i.e., the Generic Set Reaction Method (GRSM; (Carruthers, Stocker, Ellis, Seaton, & Smith, 2017); (Stocker, et al., 2023)). This Technical Support Document (TSD) reviews the scientific merit, implementation of the GRSM formulation, and summarizes selected model evaluations to support the application of GRSM as a Tier 3 NO_2 screening option for use as part of the proposed regulatory version of AERMOD.

2. Background

The chemistry, regulatory status, and performance evaluations of all existing AERMOD NO_2 screening options are discussed in the U.S. EPA TSD for NO_2-Related AERMOD Options and Modifications (U.S. EPA, 2015, December). This TSD will discuss the chemistry, proposed regulatory status, and model behavior and performance of GRSM. Following the 2015 TSD, selected graphical and statistical (U.S. EPA, 1992) comparisons between GRSM and other NO_2 regulatory options are presented.

2.1 The 3-Tiered Approach for AERMOD NO_2 Modeling Demonstrations

Section 4.2.3.4 of Appendix W (2017) details a 3-tiered approach for evaluating the modeled impacts of NO_X emission sources. These tiers assume increasing levels of conservatism (i.e., conservation of air quality as a resource for protecting public health) in the assessment of hourly and annual average NO_2 impacts from point, volume, and area sources for the purposes of supporting the PSD program, SIP planning, and transportation general conformity. The 3-tiered approach addresses the co-emissions of NO and NO_2 and the subsequent conversion of NO to NO_2 in the atmosphere. The tiered levels include:

- Tier 1 – assuming that all emitted NO is converted to NO_2 (full conversion),
- Tier 2 – using the Ambient Ratio Method 2 (ARM2), which applies an assumed equilibrium ratio of NO_2 to NO_X, based on analysis of and correlation with nationwide hourly observed ambient conditions (Podrez, 2015), and
- Tier 3 – applying the Ozone Limiting Method (OLM; (Cole & Summerhays, 1979)) and Plume Volume Molar Ratio (PVMRM; (Hanrahan, P.L., 1999a and 1999b)) screening options based on site-specific hourly ozone data and source-specific NO_2 to NO_X in-stack ratios.

As discussed in section 4.2.3.4(e), regulatory application of Tier 3 screening options shall occur in consultation with the EPA Regional Office and appropriate reviewing authority.

[1] For more information on the proposed revisions to Appendix W and updates to AERMOD, please reference: https://www.epa.gov/scram/2023-appendix-w-proposed-rule

3. Current Regulatory Status and Features of GRSM

As part of the 2023 proposed revisions to the Guideline, the EPA is proposing to include the GRSM as a regulatory non-default Tier 3 NO_2 screening option in AERMOD version 23132.

Following peer-reviewed publication (Carruthers, Stocker, Ellis, Seaton, & Smith, 2017), GRSM was added to AERMOD as an alpha option in version 21112 and later updated to a beta option in version 22112. The GRSM option is proposed to be adopted as a beta option in AERMOD version 23132, and later advanced to a full regulatory NO_2 screening option upon release of the 2024 version of AERMOD.

The primary motivation behind the formulation and development of the GRSM NO_2 screening option is to address photolytic conversion of NO_2 to NO and to address the time-of-travel necessary for NO_X plumes to disperse and convert the NO portion of the plume to NO_2 via titration and entrainment of ambient ozone. The current regulatory non-default Tier 3 NO_2 screening options, PVMRM and OLM, do not address or provide for treatment of these photolysis and time-of-travel mechanisms, and have been shown to over-predict for some source characterizations and model configurations at project source ambient air boundaries and within the first 1-3 km. (Stocker, et al., 2023) and as presented in this TSD.

4. GRSM Implementation in AERMOD

The functionality of the GRSM code implementation in AERMOD is similar to that of the PVMRM and OLM schemes, with exception to some additional input requirements necessary for treatment of the reverse NO_2 photolysis reaction during daytime hours. Modeled source inputs for GRSM require NO_2/NO_X in-stack ratios, with similar assumptions as applied to PVMRM and OLM pursuant to section 4.2.3.4 of the *Guideline*. Ambient model inputs for GRSM require hourly ozone concentrations taken from an appropriately representative monitoring station or selection of monitoring stations for varying upwind sector concentrations. GRSM also requires hourly NO_X concentration inputs to resolve the daytime photolysis of NO_2 reaction in equilibrium with ozone titration conversion of the NO portion of the NO_X plume. Hourly NO_X and NO_2 concentrations input to AERMOD when using the GRSM method can also vary by upwind sector concentration, as appropriate. Background NO_2 concentrations are accounted for in the GRSM daytime equilibrium NO_2 concentration estimates based on the chemical reaction balance between ozone entrainment and NO titration, photolysis of NO_2 to NO, and ambient background NO_2 participation in titration and photolysis reactions. Nighttime NO_2 estimates from GRSM are based on ozone entrainment and titration of available NO in the NO_X plume, and by default, AERMOD sets nighttime ozone concentrations to 40 parts per billion (ppb) unless the NOMINO3 model option is specified. Note that all hourly ozone and NO_X ambient inputs to GRSM must coincide with the hourly meteorological data records for the

period of the modeling analysis (i.e., minimum of 1-year for on-site data, 3 years of prognostic data, and 5 years of airport data (i.e., meteorological data collected by either the National Weather Service (NWS) or the Federal Aviation Administration (FAA), typically at airport locations).

Updates to the GRSM formulation in AERMOD version 22112 were completed in late 2022 to address more realistic building effects on instantaneous plume spread, accounting for multiple plume effects on entrainment of ozone, and the tendency of GRSM to over-predict in the near-field (e.g., beyond approximately 0.5 km to 3 km for typical point source releases). Sensitivity testing and model performance evaluations of these updates to GRSM in AERMOD version 23132 have shown consistent or improved model behavior and performance. Please see Appendix A for model evaluation and sensitivity testing results comparisons between GRSM code implementations in AERMOD versions 22112 and 23132. The model performance evaluations of GRSM specific to AERMOD version 23132 and compared to other regulatory NO_2 options are presented and discussed in the following sections.

5. Model Evaluation of GRSM

Statistical evaluation of GRSM NO_2 model performance was conducted based on four source-oriented ambient ozone and NO_2 monitoring databases assuming rural dispersion conditions. Two legacy (1993) databases reflect the ARM2, OLM, and PVMRM evaluations presented in the 2015 TSD for NO_2 modeling options (U.S. EPA, 2015, December). These legacy databases included 1-year datasets developed for a power plant located on the island of Moloka'i, Pala'au, Hawaii (Pala'au), and for a gas processing plant located in Artesia, New Mexico (Empire Abo). Details of the Pala'au and Empire Abo databases are discussed at length in a 2013 technical report (RTP Environmental Associates, Inc., 2013). The other two evaluation databases were developed more recently in the 2014-2016 time period and include a 1-year field study at a gas compressor station facility located near Balko, Oklahoma (Balko), and a six-week field study at an oil and gas drill rig installation located in the Denver-Julesburg Basin near Platteville, Colorado (Colorado). The Balko database included ozone and NO_2 data collected at four monitoring stations from December 2015 through December 2016. Details on the development of the Balko database were published in March of 2020 (Panek, 2020) along with model observation comparisons with ARM2, PVMRM, and OLM. The Colorado database included data collected at a total of 12 monitoring locations upwind and downwind of two oil and gas well drilling pads for a five-week period October 10th through November 16th, 2014. Further details on the Colorado database are available at EPA's SCRAM website and documented in a separate TSD (Colorado Field Study Workgroup: ERM, 2020).[2] All four model evaluation databases

2 Denver-Julesburg Bason, Colorado NO2 Evaluation Database: https://gaftp.epa.gov/Air/aqmg/SCRAM/models/preferred/aermod/eval_databases/denver-julesburg.zip

included site-specific meteorological data collected at the site, re-processed with AERMET version 23132. Summaries of all databases and performance model evaluations are also discussed in a technical report authored by the developers of GRSM for AERMOD (Stocker, et al., 2023).

As discussed previously in Section 4.3 of (RTP Environmental Associates, Inc., 2013), conversion of NO_2 and NO_X measurements in ppb to micrograms per cubic meter ($\mu g/m^3$) requires careful consideration of the actual and standard meteorological conditions as well as the separate contributing constituent components of the NO_X plume in terms of NO and NO_2 ppb by volume. Conversion of ppb to $\mu g/m^3$ from actual to standard temperature and pressure conditions generally increases measurement concentrations by approximately 10% depending on season, climatology, and elevation. Additionally, this conversion, typically based on the conventional assumption that all NO_X is NO_2 with a molecular weight of 46 grams/mole, would increase the $\mu g/m^3$ measurement estimates by 20-30% for some shorter source-receptor distances, especially between 10's to 100's of meters and possibly as far away as approximately 3 km depending on dispersion conditions. The "true" NO_X plume at these shorter distances is composed of mostly NO (e.g., 50-95% NO/NO_X by volume) and therefore, would contain less mass given the 30 g/mole molecular weight of NO, which accounts for the 20-30% conservative estimates of NO_X as NO_2 emission inputs typically used in AERMOD NO_2 demonstrations. As such, and based on the most current information on the four field datasets considered in this TSD, the NO_X as NO_2 assumption was applied to all NO_X emissions inputs, thereby introducing a conservative bias in the modeled mass emission rates. From a regulatory perspective, the performance of this conservative NO_X as NO_2 emissions assumption when compared to actual measured NO_X concentrations was considered because a regulatory modeling result would need to show some level of performance as it pertains to the Appendix W requirement that the model does not show bias to underpredict. Therefore, all input emissions assume NO_X as NO_2 (based on most current understandings of emission factors applied), and any dispersion performance indicated from NO_X modeled compared to NO_X measured assumes no change to the modeled $\mu g/m^3$ concentrations whereas measured NO_X represents the actual $\mu g/m^3$ concentrations (at standard temperature and pressure; STP) as would be the case for any regulatory modeling or monitoring demonstration. Note that AERMOD NO_X and NO_2 concentrations in $\mu g/m^3$ are calculated internally based on standard temperature and pressure (i.e., 298.15 K and 1013.25 mb). Chemistry performance was assessed in terms of modeled $\mu g/m^3$ NO_2 at STP compared to measured $\mu g/m^3$ NO_2 (after conversion from ppb to $\mu g/m^3$ at STP).

5.1 Pala'au, Hawaii NO_2 Database

The Pala'au hourly NO_2 and ozone data were collected at a monitoring station located

approximately 220 meters northwest of the facility. Hourly varying ozone data was developed from the on-site monitoring data (93% complete). The annual ozone substitution value was set to the default 40 ppb for all NO_2 models. A single annual NO_X value was set to 2.5994 $\mu g/m^3$ for the model simulations using GRSM. Background NO_2 assumed 0.69838 ppb for all conversion methods. NO_X emissions were assumed to be non-varying for the entire 1993 study period, and included six diesel engines and one combustion turbine with emission rates ranging from an average of 12.6 lb/hr to a maximum of 27 lb/hr; total NO_X emissions of 88.3 lb/hr. All sources assumed NO_2/NO_X in-stack ratios of 10%. Stack heights at the power plant were relatively short and range from 24-32 feet and were modeled assuming flat terrain. All NO_2 model outputs were based on 1-hour averages as predicted at the single monitor receptor location.

AERMOD performs well at Pala'au as indicated in the Q-Q ranked plot shown in Figure 1 where the modeled versus observed NO_X concentrations track the 1:1 line throughout the ranked distribution. As previously discussed, modeled mass emission rates assumed all NO_X was NO_2, thus, introducing a conservative emission estimate bias that could be influencing the agreement between observed and modeled NO_X concentrations. Another emissions uncertainty for Pala'au, which could inadvertently bias model-observation agreement during non-operating periods, is the non-varying emission rates assumed for the 1-year evaluation period. However, given the proximity of the monitoring station located 220 meters northwest of the power plant, and the relatively consistent distribution of the NO_X concentrations throughout the monitoring period, altogether, these factors would indicate that the power plant operated continuously at a normal demand load for the entire year. Note that no filtering of the NO_X observations was conducted (e.g., by downwind sector) to determine the final set of 7,856 model-observation pairings shown in Figure 1.

Figure 2 shows a ranked Q-Q plot of modeled versus observed NO_2 concentrations for modeling scenarios that use the proposed GRSM NO_2 Tier 3 option as well as the other Tier 2 (ARM2) and 3 (OLM, PVMRM) regulatory NO_2 options available in AERMOD. The ARM2 option performs as intended the most conservatively, whereas OLM becomes the less conservative option by comparison. PVMRM shows some slight underprediction whereas GRSM maintains a slightly conservative performance trend just above the 1:1 line for most of the ranked distribution. GRSM performs consistently compared to the other AERMOD NO_2 options and shows no unacceptable bias to underpredict peak concentrations for the Pala'au database.

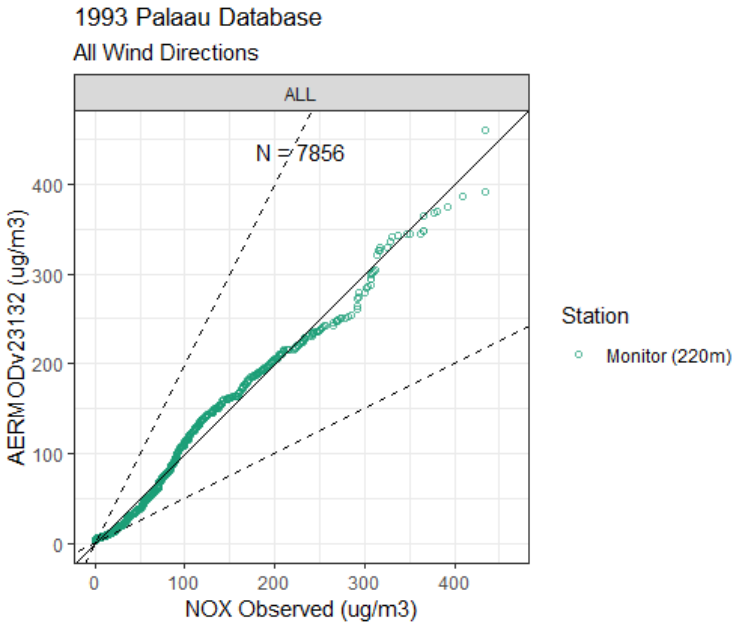

Figure 1 – Pala'au NO_X Ranked Q-Q Plot

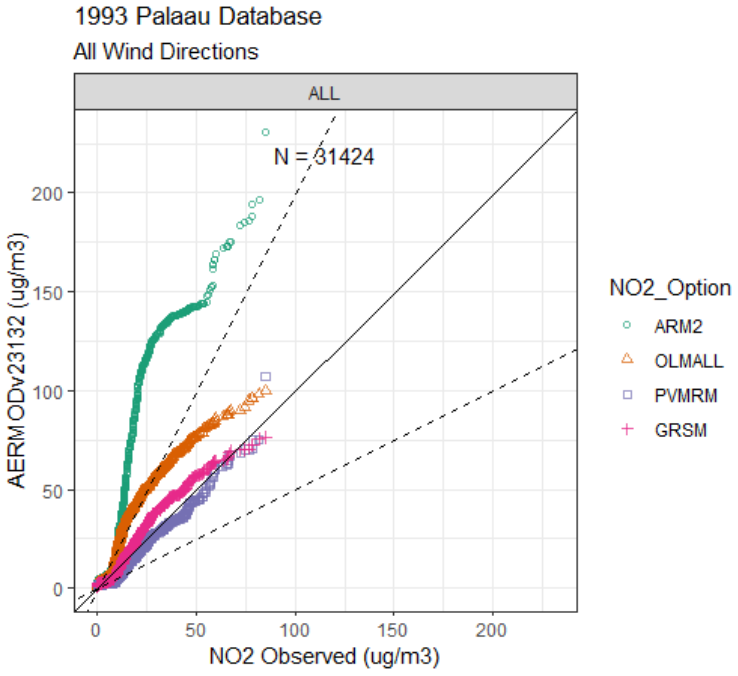

Figure 2 – Pala'au NO_2 Ranked Q-Q Plot

Table 1 shows a summary of fractional bias (FB) and robust highest concentration (RHC) model performance statistics for the NO_X and NO_2 model option scenarios evaluated for Pala'au. The FB shows decreasing conservative agreement between observations and model outputs for NO_X, ARM2, OLM, PVMRM, and GRSM model options; note that negative FB indicates a conservative bias for the option, or overprediction. The RHC ratio and RHC FB results show similar conservative hierarchy across the NO_2 option evaluations, with increasing conservatism shown for GRSM, PVMRM, OLM, ARM2, and full conversion NO_X runs.

Table 1 – Pala'au Model Performance Statistics Summary (µg/m³)

Model Opt.	FB	RHC_Obs	RHC_Mod	RHC_ratio	RHC_FB
NO_X	-1.01763	456.5125	471.9136	1.033737	-0.03318
ARM2	-1.22483	90.9536	237.2565	2.608545	-0.89152
OLM	-1.00706	90.9536	103.8257	1.141523	-0.13217
PVMRM	-0.79509	90.9536	98.17854	1.079436	-0.0764
GRSM	-0.90174	90.9536	82.87393	0.911167	0.092962

5.2 Empire Abo, Artesia, New Mexico NO_2 Database

The Empire Abo hourly NO_2, ozone, and meteorological data were collected at two monitoring stations located approximately 1.6 km northeast (north station) and 2.4 km southeast of the gas processing facility from June 11, 1993 through June 10, 1994. Model inputs for hourly ozone and background NO_2 and NO_X were based on two wind sectors starting at 100 and 280 degrees, which AERMOD interprets as downwind or flow vector wind directions. The first sector (winds blowing towards 100-280 degrees) used upwind hourly ozone and NO_2 concentrations from the north station, while the second sector (winds blowing towards 280-100) used upwind data from the south station. Substitution values for missing hourly ozone and NO_X data were taken from season-hourly varying maximum, while NO_2 season-hourly values were developed from highest-3rd-high observed values. The highest-3rd-high was selected for NO_2 substitution values in order to reflect a median value between unreasonably high maximum NO_2 values and the 1-hour NAAQS highest-8th-high. Similar to Pala'au, NO_X emissions for Empire Abo were assumed to be non-varying for the entire study period, and included 21 combustion sources with emission rates ranging from an average of 20.2 lb/hr to a maximum of 69.4 lb/hr, and with a facility total of 423 lb/hr. All sources assumed NO_2/NO_X in-stack ratios of 20%. Stack heights at the power plant from dominant sources averaged about 30 feet and all sources were modeled assuming flat terrain. All NO_X and NO_2 model outputs were based on 1-hour averages as predicted at the north and south monitor receptor locations.

As shown in the ranked Q-Q plot in Figure 3, modeled NO_X concentrations at the north and south monitors tend to overpredict; note the north monitor shows some underprediction for

the lower half of the ranked distribution. As previously mentioned, the overpredictions may be in part due to the NO_X mass emission rates that assume all NO_X has converted to the mass of NO_2. Given the 1.6 km and 2.4 km distances to the north and south monitors, respectively, this assumption may be valid for most worst-case scenarios; however, the ambient monitoring data at these stations indicates the inner quartile range of the ambient NO_2/NO_X ratios varies between 66-86%. The non-varying hourly emissions from Empire Abo dispersed over these longer distances may also play a role in overestimating NO_X concentrations. Note that pre-filtering of the NO_X observations was not conducted (e.g., by downwind sector, or other parameter) to determine the final set of 16,547 model-observation pairings shown in Figure 3.

Figures 4 and 5 show ranked Q-Q plots of modeled versus observed NO_2 concentrations at the north and south monitors, respectively, for modeling scenarios that use the proposed GRSM NO_2 Tier 3 option as well as the other Tier 2 (ARM2) and 3 (OLM, PVMRM) regulatory NO_2 screening options available in AERMOD. Similar to the results at Pala'au, the ARM2 option performs the most conservatively, whereas OLM and GRSM modeled concentrations track closely together and are more conservative than PVMRM. GRSM performs consistently compared to the other AERMOD NO_2 options and shows no unacceptable bias to underpredict peak concentrations for the Empire Abo database.

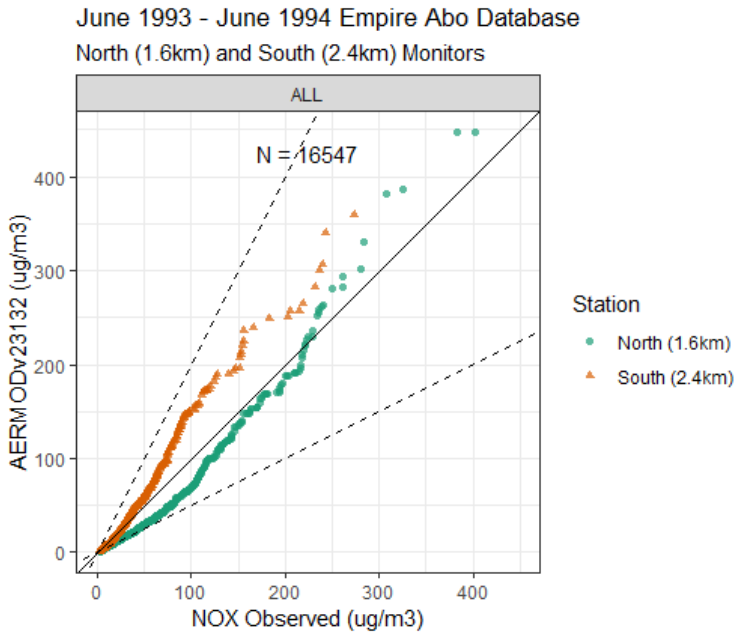

Figure 3 – Empire Abo NO_X Ranked Q-Q Plot

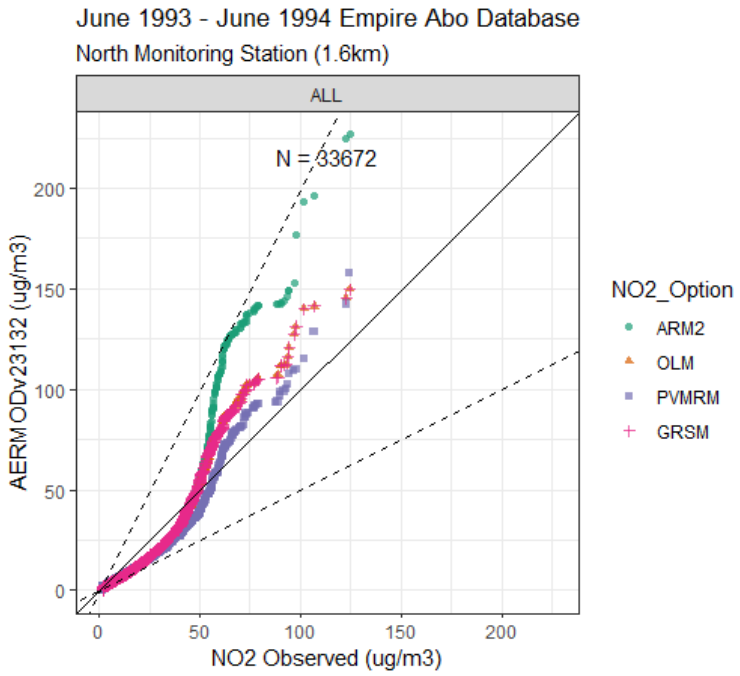

Figure 4 – Empire Abo NO_2 Ranked Q-Q Plot for the North Monitor

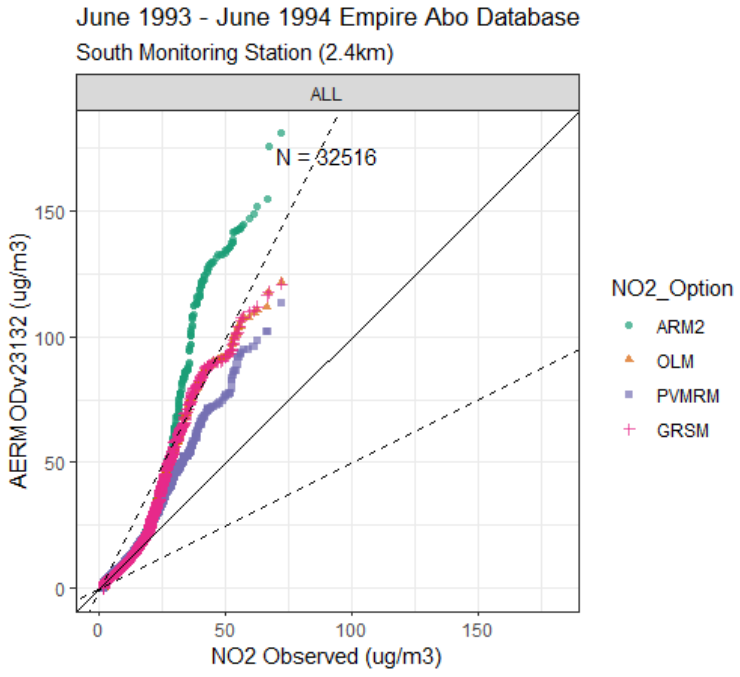

Figure 5 – Empire Abo NO_2 Ranked Q-Q Plot for the South Monitor

Table 2 shows summary model performance statistics for NO_X and NO_2 at the Empire Abo north and south monitors. The FB shows conservative agreement between observations and model outputs. The RHC ratio and RHC FB show conservative bias for the north monitor and south monitor, with the most conservatism shown for NO_X and ARM2, whereas OLM, PVMRM, and GRSM display consistent conservative bias for the north and south monitors.

Table 2 – Empire Abo Model Performance Statistics Summary (µg/m³)

Station	Model Opt.	N	FB	RHC_Obs	RHC_Mod	RHC_ratio	RHC_FB
North (1.6km)	NO_X	8418	0.519675	356.2944	477.27	1.339538	-0.29026
	ARM2	8418	0.289203	130.2695	204.0459	1.566337	-0.44136
	OLM	8418	0.292575	130.2695	152.6254	1.171613	-0.15805
	PVMRM	8418	0.354584	130.2695	141.475	1.086018	-0.08247
	GRSM	8418	0.314298	130.2695	152.9922	1.174428	-0.16044
South (2.4km)	NO_X	8129	0.364385	323.4253	392.8127	1.214539	-0.19375
	ARM2	8129	-0.00239	72.57853	172.0086	2.369966	-0.81304
	OLM	8129	0.000409	72.57853	128.2316	1.766798	-0.55429
	PVMRM	8129	0.045474	72.57853	121.1714	1.669522	-0.5016
	GRSM	8129	0.01555	72.57853	129.4047	1.782962	-0.56268

5.3 Balko, Oklahoma NO_2 Database

The 1-year of hourly NO_2 observations records for each of the four monitoring stations were reduced by excluding values collected during hours when NO_X concentrations were below 20 ppb and when the downwind direction from the source to the monitoring receptor location was more than approximately 20-30 degrees (i.e., assuming a 40-60-degree downwind sector of influence). As such, non-missing hourly modeling results were paired in time with the reduced observations (total N pairs = 1742) to generate ranked Q-Q plots and summary statistics. In brief, the monitoring stations, distances, and downwind directions from the sources were: Field 425 m, 360 deg; North Fence (NF) 140 m, 360 deg; East Fence (EF) 101 m, 68 deg; and Tower 66 m, 246 deg. NO_X emissions at Balko were dominated by two of the large 2-stroke cycle lean-burn natural gas-fired engines with combined maximum hourly NO_X emission rates on the order of 120 lb/hr and NO_2/NO_X in-stack ratios of 10%. Relatively short stacks for these units were modeled at 10 m and 20 m, with adjacent dominant building heights at 11-13 m. For further details on the Balko field study and model configurations see (Panek, 2020).

The NO_X and NO_2 Q-Q plots shown in Figure 6 represent all model-observation data pairs from the four monitoring stations. Both NO_X and NO_2 predictions using OLM and GRSM trend below the 1:1 line at the upper end of the concentration distributions, but above the 1:2 line. NO_2 predictions using ARM2 performs above the 2:1 line through the first half of the ranked

distribution, converging to the 1:1 line at the upper end of the distribution. The negative bias shown in the NO_X performance suggests dispersion assumptions such as downwash and stack parameters could be refined for some monitoring locations. The negative bias in NO_X is largely driven by the model performance and higher observed NO_X impacts at the North Field (NF) monitor, which is well within the near wake zone of two adjacent end-to-end, long buildings. As shown in Figure 7, all other monitor locations show more conservative, or positive bias for NO_X.

The ranked Q-Q plot panels for NO_X and NO_2 shown in Figure 7 are presented for each monitor location. NO_X model predictions at the Field and East Fence show conservative bias with peak value data pairs falling between the 2:1 and 1:1 lines. NO_2 model predictions at these stations ranging from 175 µg/m^3 to 200 µg/m^3 show a consistent conservative hierarchy across the NO_2 options decreasing in order of the ARM2, OLM, PVMRM, and GRSM options. The NO_X predictions at the meteorological Tower monitor fall mostly along the 1:1 line; however, PVRM is the least conservative performing NO_2 option at this predominantly southwesterly, upwind location. NO_X predictions at the North Fence follow the 1:1 line with negative bias trends starting at 750 µg/m^3 and ending above the 1:2 line at about 1600 µg/m^3. The negative bias at the upper part of the distribution is most likely influenced by uncertainties in source and building downwash characterizations at what is a relative short downwind 140-meter distance from the dominant stack. The conservative hierarchy shown for NO_2 predictions at the North Fence is similar to the other monitor locations; however, the overly conservative PVMRM predictions for the last three data pairs suggest further uncertainties in instantaneous plume and building downwash formulations coded for PVMRM. GRSM does not mimic this behavior.

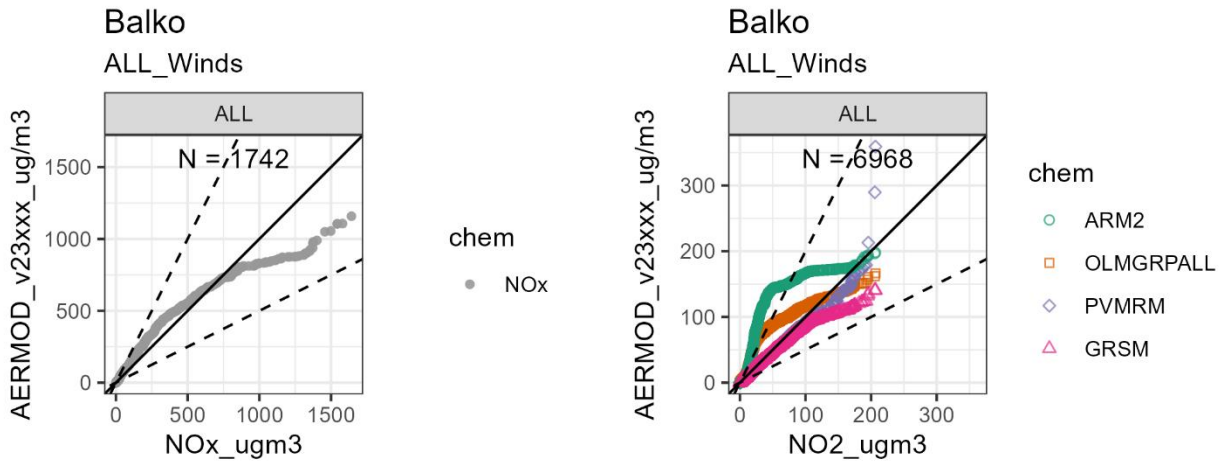

Figure 6 – Balko NO_X and NO_2 Ranked Q-Q Plot for all monitors

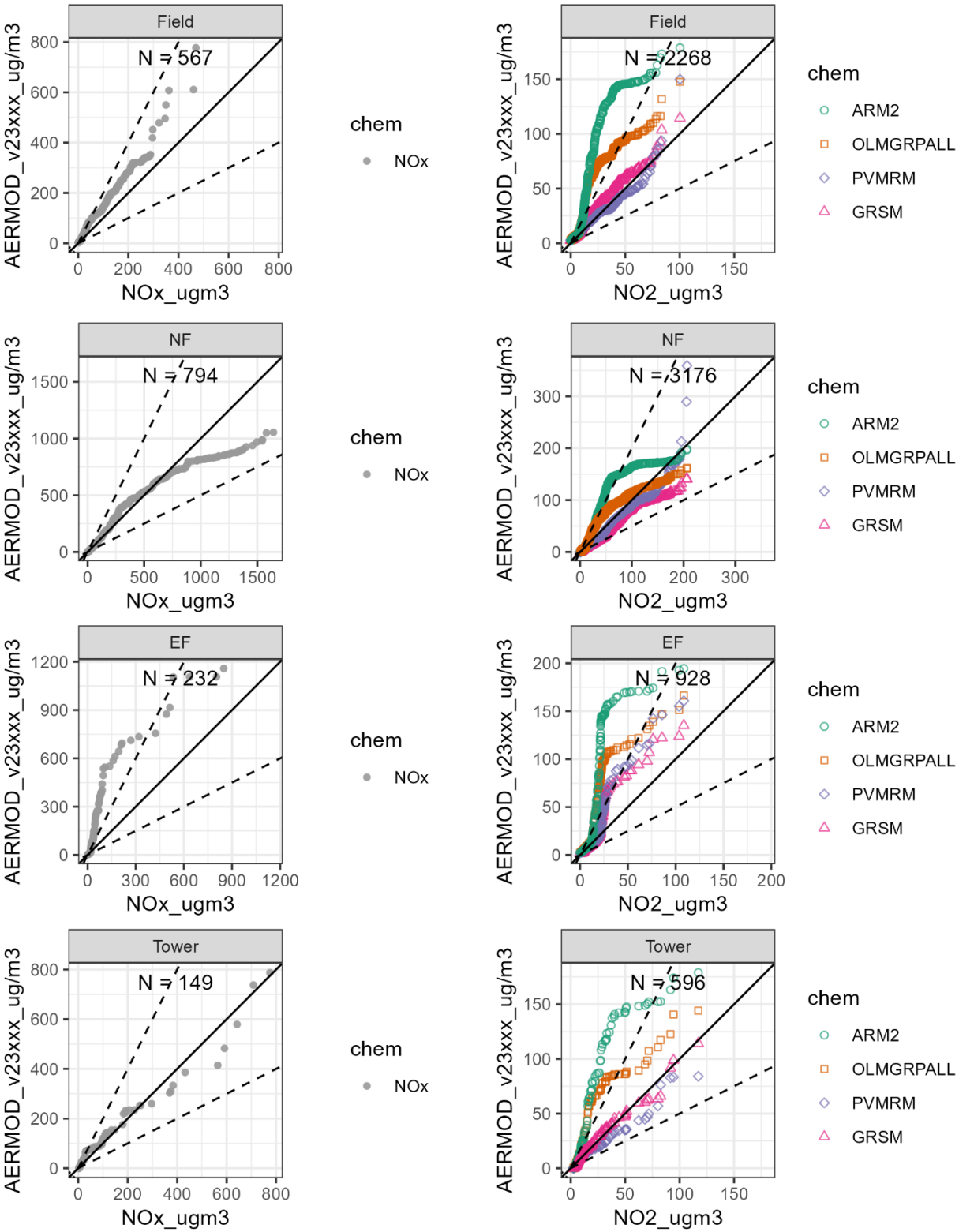

Figure 7 – Balko NO_X and NO_2 Ranked Q-Q Plot by monitor

Table 3 provides FB and RHC statistics calculated for all monitor locations and for all NO_2 model options evaluated including NO_X, ARM2, OLM, PVMRM, and GRSM. The table is sorted by model option and decreasing RHC ratio values. In all, the GRSM RHC ratio and RHC FB results indicate more consistent, logical model behavior when compared with modeled NO_X performance at the four monitors. With exception to the uncertainties discussed at the NF monitor, GRSM performance statistics show less conservative bias than the other NO_2 model options.

Table 3 – Balko Model Performance Statistics Summary (µg/m³)

Station	Model Opt.	N	FB	RHC_Obs	RHC_Mod	RHC_ratio	RHC_FB
EF	NO_X	232	-0.30893	785.1347	1449.214	1.845816	-0.59443
Field	NO_X	567	-0.33405	481.5579	637.3523	1.323521	-0.27848
Tower	NO_X	149	0.050238	825.8741	719.8355	0.871604	0.137204
ALL	NO_X	1742	-0.13172	1884.88	1162.402	0.616698	0.474179
NF	NO_X	794	0.030388	1884.88	1069.941	0.567644	0.551599
EF	ARM2	232	-0.5797	106.2721	210.4881	1.980653	-0.65801
Tower	ARM2	149	-0.23291	121.7104	211.9201	1.741183	-0.54078
Field	ARM2	567	-0.67069	104.2684	171.3581	1.643433	-0.48682
ALL	ARM2	1742	-0.44312	220.7673	199.6457	0.904326	0.100481
NF	ARM2	794	-0.28016	220.7673	191.5234	0.867535	0.141861
EF	OLMGRPALL	232	-0.51368	106.2721	164.5996	1.548851	-0.43067
Field	OLMGRPALL	567	-0.59014	104.2684	130.0644	1.2474	-0.22017
Tower	OLMGRPALL	149	-0.16588	121.7104	137.5235	1.129924	-0.122
ALL	OLMGRPALL	1742	-0.34007	220.7673	172.0811	0.779468	0.247863
NF	OLMGRPALL	794	-0.14346	220.7673	169.5039	0.767794	0.262707
EF	PVMRM	232	-0.14628	106.2721	192.0816	1.807451	-0.57522
NF	PVMRM	794	0.17654	220.7673	269.9143	1.222619	-0.20032
ALL	PVMRM	1742	0.048435	220.7673	259.2444	1.174288	-0.16032
Field	PVMRM	567	-0.11716	104.2684	110.9297	1.063887	-0.06191
Tower	PVMRM	149	0.299099	121.7104	92.84917	0.76287	0.269028
EF	GRSM	232	-0.11145	106.2721	147.6259	1.389132	-0.32575
Field	GRSM	567	-0.26831	104.2684	105.8487	1.015156	-0.01504
Tower	GRSM	149	0.217114	121.7104	104.3644	0.857481	0.153454
ALL	GRSM	1742	0.034885	220.7673	142.8789	0.647192	0.428375
NF	GRSM	794	0.259959	220.7673	138.3798	0.626813	0.458796

5.4 Denver-Julesburg Basin, Platteville, Colorado NO_2 Database

The Colorado NO_2 database is comprised of twelve monitors deployed for roughly six weeks (October 10 – November 16, 2014) at two adjacent oil and gas drilling installations, Pads 1 and

2 outside Platteville, CO. At Pad 1, the six upwind (southeast) and six downwind (northwest) monitors were positioned around the pad on which the emission sources included a drill rig, five generators, and one small boiler. Similarly, at Pad 2, six monitors upwind and six downwind were located around the pad with the same emission sources. The monitors were re-positioned at Pad 2 on three separate occasions to capture NO_X emissions during changing wind patterns for the last three weeks of the monitoring period. Monitor locations for both Pad 1 and 2 were placed approximately 50-100 m away from the drill rig and support generators. Hourly varying NO_X emissions were modeled for the five diesel-fired support generators and standby boiler at Pads 1 and 2 during the six-week study period. NO_X hourly emission rate totals at both pads range from roughly 10 lb/hr to 20 lb/hr with stack release heights at 18 ft just at or above the 18 ft high drill rig and 30 total adjacent and nearby buildings. Non-missing hourly modeling results were paired in time with the available observations at Pads 1 and 2 (total N pairs = 1473) to generate ranked Q-Q plots and summary statistics. All five generators show relatively equal contribution to total NO_X emissions when operating at Pads 1 and 2. The standby boiler contributions to total NO_X emissions appear to be negligible. The generator operating loads varied between approximately 50-100% load throughout the study periods at Pad 1 and 2. For further details on the Colorado field study monitor locations, hourly emission rates and operating scenarios, background hourly ozone and NO_X data wind sector filtering, and other model configurations see (Colorado Field Study Workgroup: ERM, 2020). Note that there were more than a dozen small adjacent buildings located within downwash near wake zones that extend between source and monitor locations at Pads 1 and 2. Downwash effects from these collections of buildings as well as non-varying in-stack NO_2/NO_X ratios assumed for the five generators likely influence model performance biases and uncertainties for this database.

Figures 8 and 9 show ranked Q-Q plots of AERMOD versus observed NO_X and NO_2 concentrations at Pads 1 and 2, respectively. NO_X model predictions at Pad 1 compare well with observations with exception to the last three data pairs showing some underprediction. At Pad 2, roughly half of the upper distribution of NO_X predictions show negative bias trending toward the 1:2 line, suggesting AERMOD may be overestimating dispersion; however, NO_X emissions and/or NO_2/NO_X ratios inputs may be underestimated perhaps related to uncertainties in the assumed non-varying in-stack NO_2/NO_X ratios during varying genset operating loads. Uncertainties in source characterization of building downwash may also be contributing to the model estimates at both Pads 1 and 2, especially attributable to movement of monitoring equipment at three different times around Pad 2. The conservative bias hierarchy for NO_2 options at Pads 1 and 2 is similar to NO_2 option performance discussed for the other three databases with exception to PVMRM. The unreasonable conservative bias shown for PVMRM at Pads 1 and 2 as it compares to ARM2 may be related to similar model

uncertainties discussed for the North Fence monitor at Balko, where enhanced downwash and entrainment effects on the ensemble plume are overestimated by PVMRM in the immediate vicinity of recirculation cavities and near wake downwash zones.

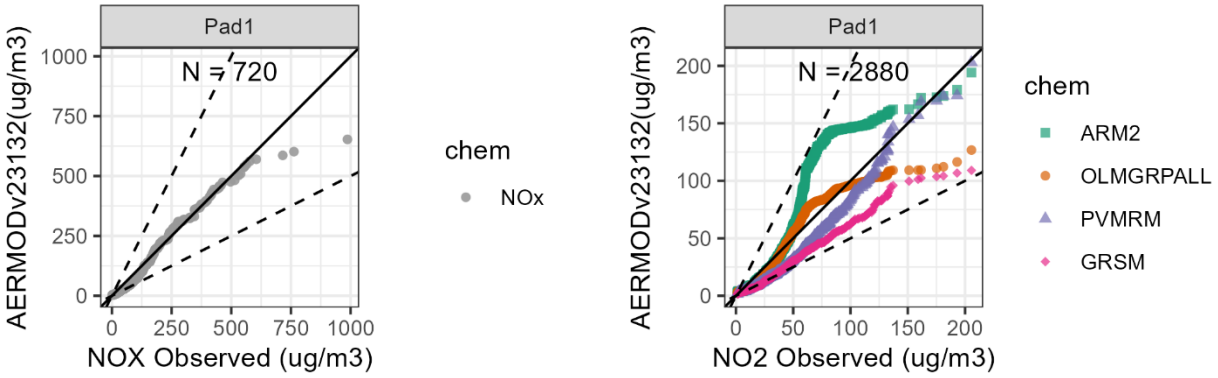

Figure 8 – Colorado NO_X and NO_2 Ranked Q-Q Plots for Pad 1

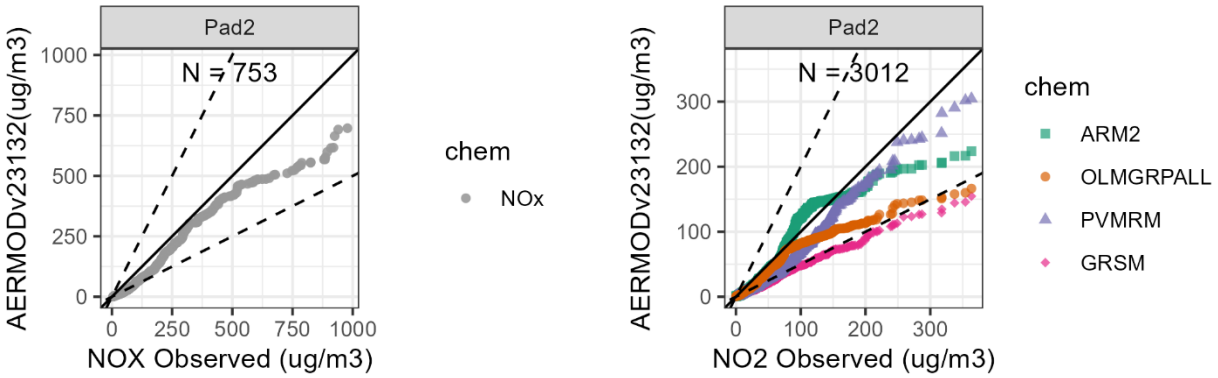

Figure 9 – Colorado NO_X and NO_2 Ranked Q-Q Plots for Pad 2

Table 4 provides summary FB and RHC statistics for all NO_2 modeled options at Pads 1, 2, and both Pads 1 and 2, sorted by model option and conservative RHC ratio. GRSM shows refined performance consistent with the ARM2 and OLM, with underpredictions most likely attributable to source characterization uncertainties. No extreme underprediction or overprediction is indicated in the RHC fractional bias values shown for GRSM at Pads 1 or 2. In general, performance for all NO_2 options seems more degraded at Pad 2 as compared to Pad 1.

Table 4 – Colorado Model Performance Statistics Summary (µg/m^3)

Pad	Model Opt.	N	FB	RHC_Obs	RHC_Mod	RHC_ratio	RHC_FB
Pad1	NO_X	720	0.315616	840.7064	734.6718	0.873874	0.134615
ALL	NO_X	1473	0.405245	1250.35	731.5125	0.585046	0.523586
Pad2	NO_X	753	0.490945	1289.554	743.2198	0.576338	0.537526
Pad1	ARM2	720	-0.02909	196.3466	185.0584	0.942509	0.059192
Pad2	ARM2	753	0.181117	388.8654	253.4506	0.65177	0.421645
ALL	ARM2	1473	0.07837	388.8343	247.755	0.637174	0.443235
Pad1	PVMRM	720	0.423036	196.3466	216.9619	1.104995	-0.09976
ALL	PVMRM	1473	0.438573	388.8343	337.1309	0.86703	0.142441
Pad2	PVMRM	753	0.45343	388.8654	335.9631	0.863957	0.145972
Pad1	OLMGRPALL	720	0.081058	196.3466	119.3968	0.608092	0.48742
Pad2	OLMGRPALL	753	0.294795	388.8654	188.1758	0.48391	0.695581
ALL	OLMGRPALL	1473	0.19032	388.8343	184.8962	0.475514	0.71092
Pad1	GRSM	720	0.525857	196.3466	121.2005	0.617279	0.473291
Pad2	GRSM	753	0.723	388.8654	180.1383	0.463241	0.733658
ALL	GRSM	1473	0.626637	388.8343	157.2032	0.404293	0.848408

6. Summary

Four NO_2 model evaluation databases were used to assess the comparative model behavior and statistical performance of GRSM. These databases represent a broad range of NO_X source characterizations, ozone and NO_X model inputs, ozone and NO_2 monitoring networks, and local and regional NO_X chemistry and meteorological environments. All database evaluations included comparisons between GRSM and all existing AERMOD Tier 1 (NO_X), Tier 2 (ARM2), and Tier 3 (OLM and PVMRM) AERMOD NO_2 regulatory screening options. Based on the ranked Q-Q plots showing NO_X and NO_2 model versus observation concentrations, and with exception to previously discussed uncertainties and degraded model performance at Pad 2 for Colorado, GRSM performs within a factor of +/- 2 range of the NO_2 observations, and thus, demonstrates no unacceptable under or over prediction biases. The statistical summaries of RHC and fractional biases for all NO_2 databases further demonstrate GRSM behaves and performs consistently in comparison with the other existing AERMOD NO_2 screening options.

References

Carruthers, D. S., Stocker, J. R., Ellis, A., Seaton, M. D., & Smith, S. E. (2017). Evaluation of an explicit NOx chemistry method in AERMOD. *Journal of the Air & Waste Management Association*, 67:6, 702-712, DOI: 10.1080/10962247.2017.1280096.

Cole, H. S., & Summerhays, J. E. (1979). A Review of Techniques Available for Estimating Short-Term NO2 concentrations. *J. Air Poll. Cont. Assoc., 29:8*, 812-817. doi:10.1080/00022470.1979.10470866

Colorado Field Study Workgroup: ERM, A. A.-W. (2020). *2014 Colorado Oil and Gas Drill Rig Field Study Model Evaluation Database - Technical Support Document.* Platteville.

Hanrahan, P. L. (1999a). The Plume Volume Molar Ratio Method for Determining NO2/NOx Ratios in Modeling - Part I: Methodology. *J. Air & Waste Manage. Assoc.*, 1324-1331.

Hanrahan, P. L. (1999b). The Plume Volume Molar Ratio Method for Determining NO2/NOx Ratios in Modeling - Part II: Evaluation Studies. *J. Air & Waste Manage. Assoc.*, 1332-1338.

Panek, J. A. (2020). PRCI ambient NO2 AERMOD performance assessment and model improvement project: Modeled to observed comparison. *Journal of the Air & Waste Management Association, Vol. 70, No. 5*, 504-521.

Podrez, M. (2015). An update to the ambient ratio method for 1-h NO2 air quality standards dispersion modeling. *Atm. Env.*, 163-170.

RTP Environmental Associates, Inc. (2013, March 3). *Ambient Ratio Method Version 2 (ARM2) for use with AERMOD for 1-hr NO2 Modeling.* Retrieved from http://www.epa.gov/ttn/scram/models/aermod/ARM2_Development_and_Evaluation_Report-September_20_2013.pdf

Stocker, J. R. (2022). #MO23 Development and Development of GRSM for NO2 Conversion in AERMOD. *Guideline on Air Quality Models: Developing the Future* (p. Conference Proceedings). Durham, NC: Air & Waste Management Association.

Stocker, J. R., Seaton, M. D., Smith, S. E., O'Neill, J., Johnson, K., Jackson, R., & Carruthers, D. (2023). *Evaluation of the Generic Reaction Set Method for NO2 conversion in AERMOD. The modification of AERMOD to include ADMS chemistry.* Cambridge Environmental Research Consultants (CERC) Technical Report.

U.S. EPA. (1992). *Protocol for Determining the Best Performing Model. EPA-454/R-92-025.* Research Triangle Park, NC: Office of Air Quality Planning and Standards.

U.S. EPA. (2015, December). *Technical support document (TSD) for NO2-related AERMOD modifications. Publication No. EPA-454/B-15-004.* Research Triangle Park, North Carolina: Office of Air Quality Planning and Standards.

Appendix A – GRSM Code Updates and Testing for AERMOD v23132

The GRSM code implemented as a beta option in AERMOD version 22112 (GRSM22112) was updated in AERMOD version 23132 (GRSM23132) to improve the performance and model behavior as dependent upon the following calculations:

- Instantaneous plume spread
- Building effects on plume spread in near-to-far wake downwash zones
- Multiple plume effects combined with building effects

This appendix provides clarifying supporting information on the improved performance and model sensitivities to these calculations as implemented in GRSM23132. The motivation for code revisions to GRSM in AERMOD version 23132 includes accounting for building effects on enhanced dispersion and entrainment of ozone and subsequent reaction with modeled NO_X emissions. Treatment of building effects addresses overpredictions for some source and downwash configurations at receptors located between near and far-wake dispersion zones out to approximately 1-3km downwind where building effected turbulence intensities approach ambient, non-building turbulence levels. Further discussion and details on the specific mathematical formulation changes and physics can be referenced in (Stocker J. R., 2022).

A.1 Model Performance Evaluation Results Summary

The GRSM23132 code updates were compared to the previous GRSM22112 code for the four model performance evaluation NO_2 databases covered in this TSD. Please refer to the text in the main body of the TSD for discussion of the specific details on each NO_2 database. This section provides side-by-side model performance comparisons between the two GRSM formulations in terms of scatter plots, ranked Q-Q plots (Figures A.1-1 through A.1-9), and a model performance statistical summary shown in Table A.1-1. Each scatter and Q-Q plot show model results from GRSM23132 and GRSM22112 for each of the four NO_2 databases to support implementation of the updated code implemented in AERMOD version 23132. Note that all four NO_2 databases include building downwash with monitor receptors at distances varying between 50m and 2.4 km, thus, providing a basis for comparing updates to the building effects formulations in GRSM23132.

The scatter plot and Q-Q plot for the Pala'au database are shown in Figure A.1-1. The scatter plot shows model-observation data pairs that are paired in time and space. This provides some indication of the general agreement between modeled and observed data while also illustrating combined uncertainties in terms of overall performance of dispersion and NO_2 chemistry predictions. The scatter plot for Pala'au indicates a wider range of model predictions with GRSM23132, with the slope of the linear model increasing closer to unity than shown for GRSM22112 concentration pairs, suggesting GRSM22112 agreement with observed NO_2 values may be lacking in statistical range. The larger statistical range of GRSM23132 concentrations carries forward to the ranked Q-Q plot, where ranked model-observation values are unpaired in time and space, and indicates better agreement between GRSM23132 predictions and observations, whereas GRSM22112 slightly underpredicts by comparison, especially at the upper range of the concentration distribution. Note the Pala'au monitor is located within the

near wake building downwash zone and improved agreement with GRSM23132 predictions at that location indicates treatment of building effects is a contributing factor. Table A.1-1 statistics indicate more favorable RHC and FB results for GRSM23132 further indicating improved performance from the treatment of building effects on near wake zone dispersion and NO_2 chemistry.

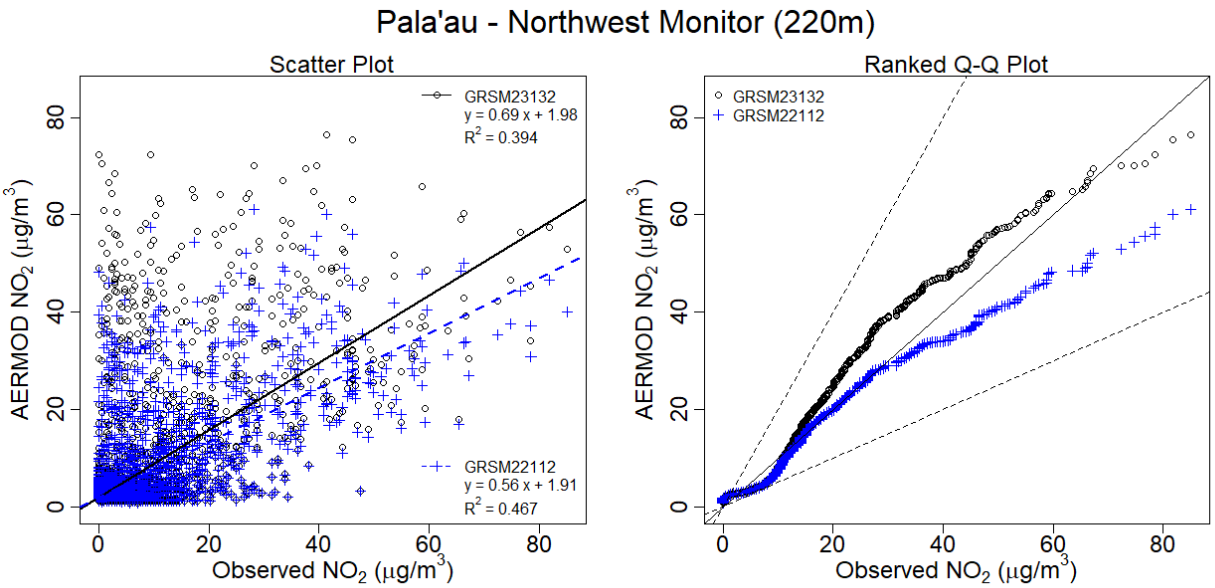

Figure Error! No text of specified style in document..**1-1 – Pala'au Monitor Scatter Plot and Ranked Q-Q Plot**

Figures A.1-2 and A.1-3 show the scatter plot and Q-Q plot for the Empire Abo NO_2 database at the North and South Monitoring stations located 1.6km northeast and 2.4km southwest, respectively. Very little difference in scatter and Q-Q plot data pairs are shown for GRSM23132 and GRSM22112 NO_2 predictions. This indicates that there is no significant difference between the performance of the GRSM code versions for the non-varying emission sources and building downwash characterizations modeled for Empire Abo at distances extending in the near field 1-3km. Table A.1-1 indicates a slight increase in fractional bias for GRSM23132. Therefore, the Empire Abo database was not found to be overly sensitive to the code updates in GRSM23132.

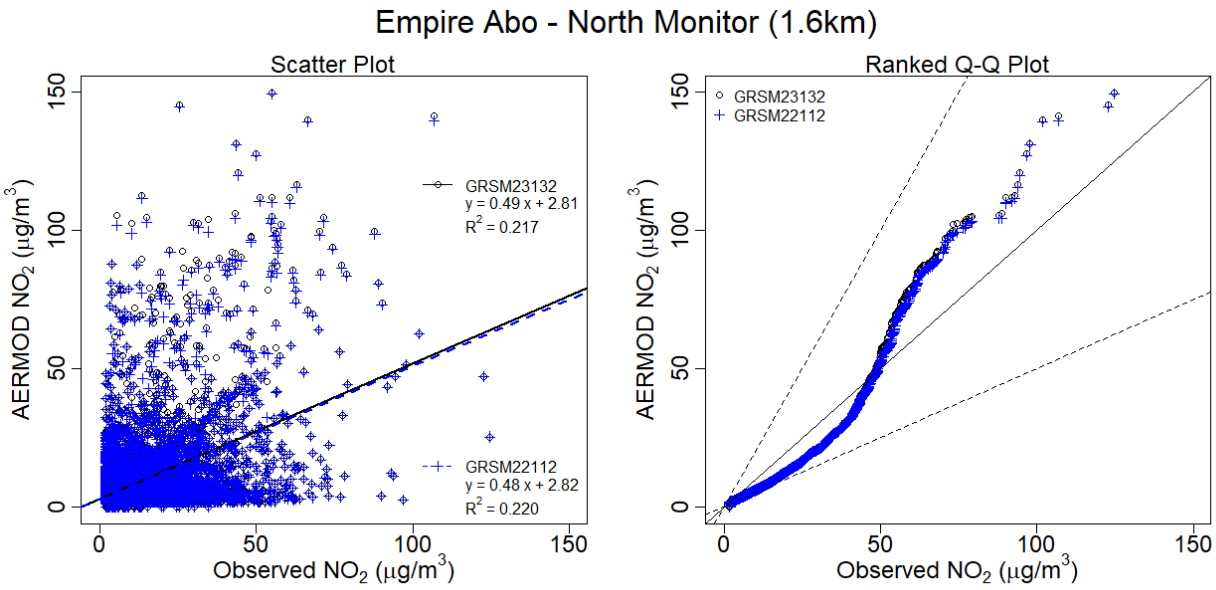

Figure Error! No text of specified style in document.**..1-2 – Empire Abo – North Monitor Scatter Plot and Ranked Q-Q Plot**

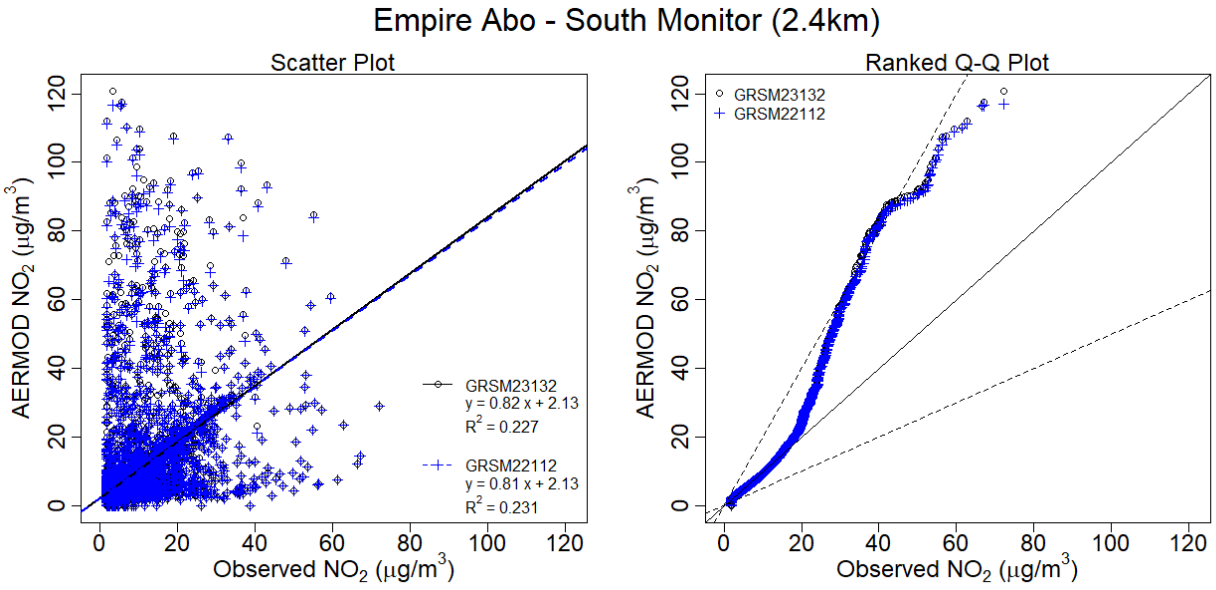

Figure Error! No text of specified style in document.**..1-3 – Empire Abo – South Monitor Scatter Plot and Ranked Q-Q Plot**

Scatter plot and Q-Q plot performance comparisons between GRSM23132 and GRSM22112 for the Balko natural gas compressor station NO_2 database are shown in Figures A.1-4, A.1-5, A.1-6, and A.1-7 for the Field, North Fence (NF), East Fence (EF), and Tower monitoring stations, respectively. Generally, the scatter plots indicate a slight increase in GRSM23132 predictions compared to GRSM22112; however, Q-Q plots show slight improvements in performance in terms of GRSM23132 predictions approaching one-to-one agreement between model-observation data pairs at the upper-end of the

concentration distribution values shown, most notably for the NF and EF monitoring receptor locations where near wake building downwash effects are expected to significantly influence model performance. This is consistent with the overall improved performance shown in Table A.1-1 for RHCs, FBs, RHC ratios, and RHC FBs at the NF, EF, and Tower receptor locations.

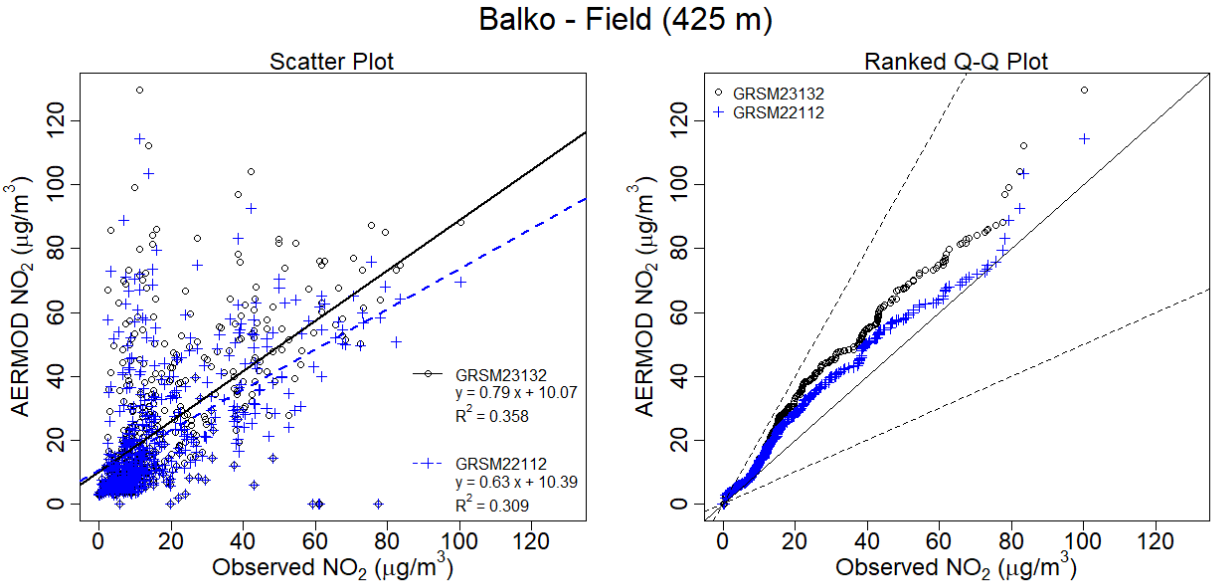

Figure Error! No text of specified style in document.**.1-4 – Balko – Field (north) Monitor Scatter Plot and Ranked Q-Q Plot**

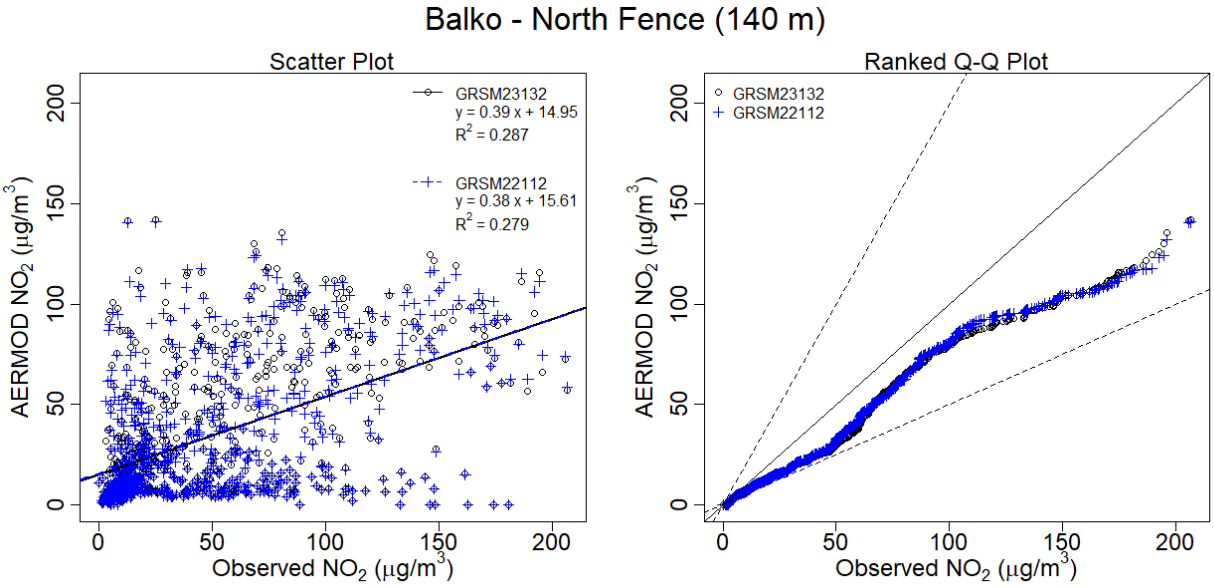

Figure Error! No text of specified style in document.**.1-5 – Balko – North Fence Monitor Scatter Plot and Ranked Q-Q Plot**

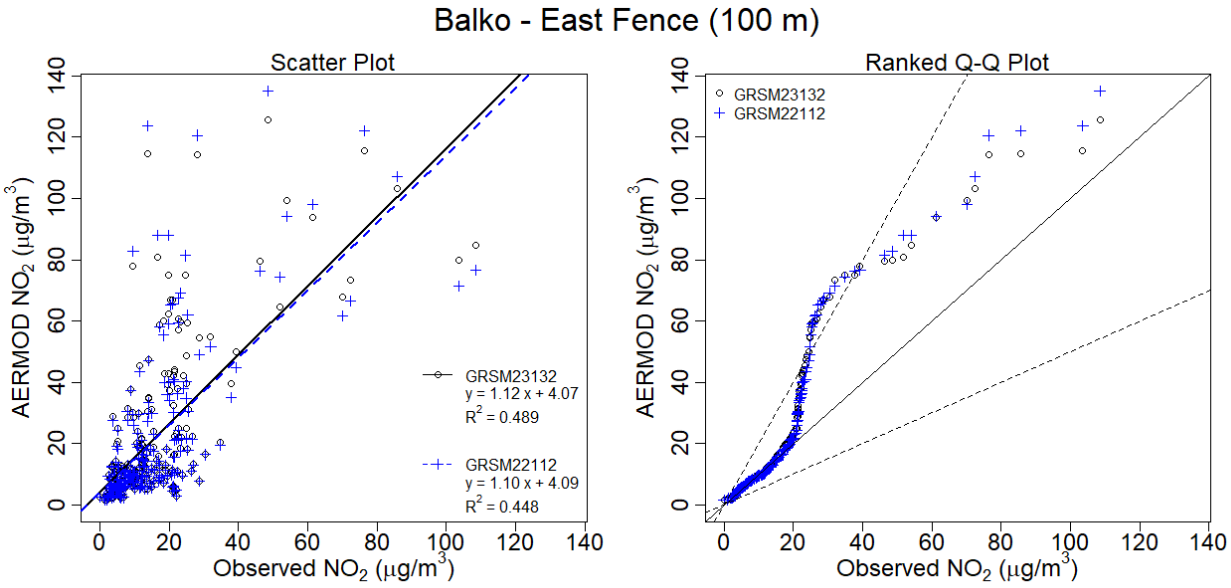

Figure Error! No text of specified style in document..**1-6 – Balko – East Fence Monitor Scatter Plot and Ranked Q-Q Plot**

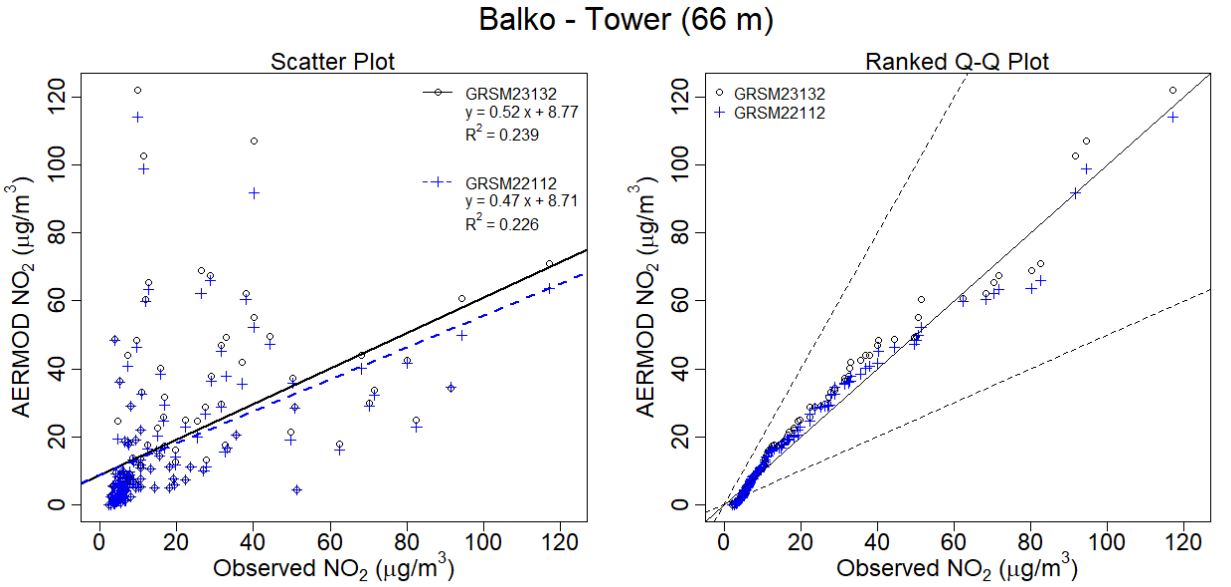

Figure Error! No text of specified style in document..**1-7 – Balko – Tower (southeast) Monitor Scatter Plot and Ranked Q-Q Plot**

Model performance improvements for the Colorado oil and gas well pad NO_2 database are indicated in comparison scatter plot and Q-Q plot Figures A.1-8 and A.1-9 for Pad 1 and Pad 2, respectively. GRSM23132 shows less tendency for underpredictions at the upper end of the concentration distribution in scatter plots and Q-Q plots for both Pad 1 and Pad 2. Statistics shown in Table A.1-1 indicate the most improvement of all four databases evaluated for Pad 1 and Pad 2 in terms of RHCs, FB, RHC FBs, and RHC ratios. The twelve monitor receptors at both Pad 1 and Pad 2 were located well within the cavity and near wake downwash zones of the well pad structures and short stacks modeled, and as

such, model performance improvements for these receptors support implementation of GRSM23132 treatment of building effects over the more simplistic treatments provided by GRSM22112.

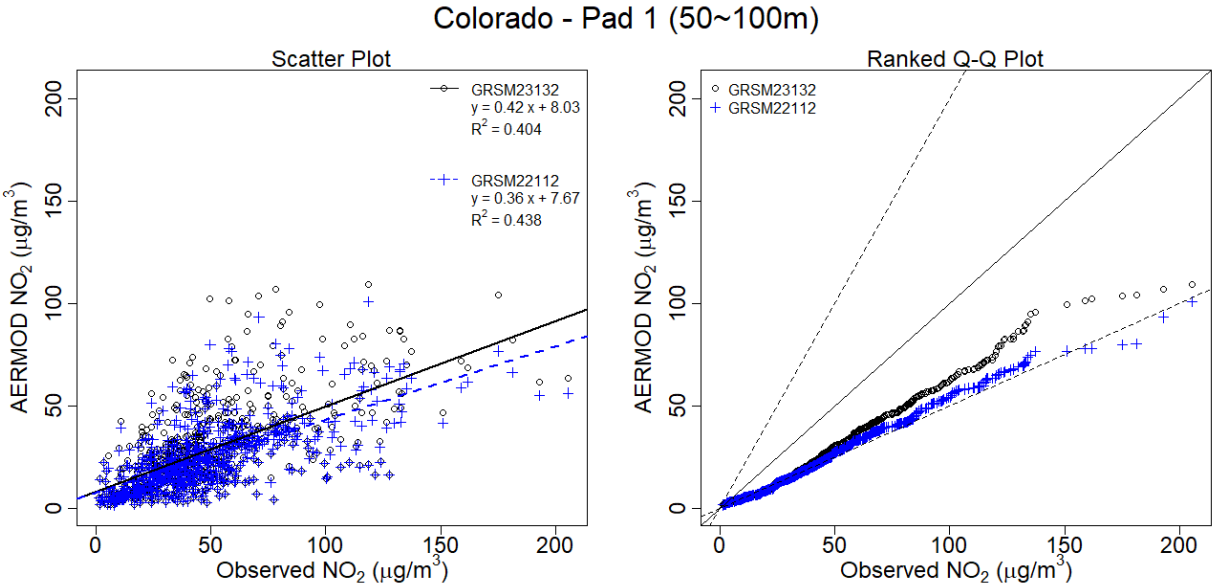

Figure Error! No text of specified style in document.**.1-8 – Colorado – Pad 1 Monitors Scatter Plot and Ranked Q-Q Plot**

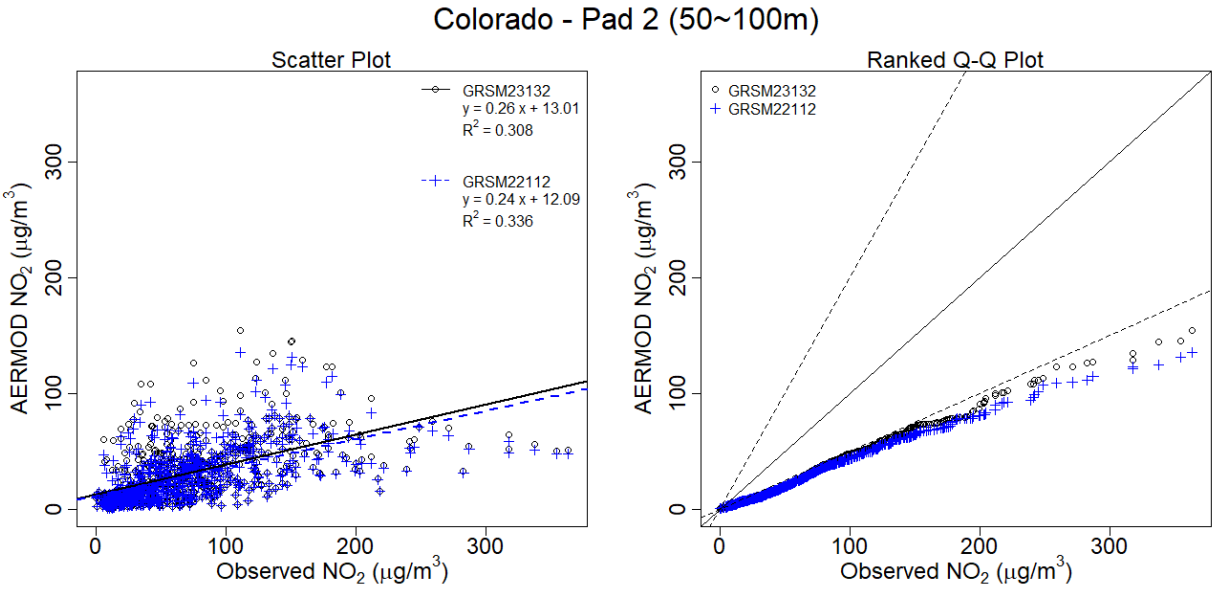

Figure Error! No text of specified style in document.**.1-9 – Colorado – Pad 2 Monitors Scatter Plot and Ranked Q-Q Plot**

Table A.1-1 – GRSM v23132 and v22112 Model Performance Statistics Summary (µg/m^3)

Statistics	Pala'au	Empire Abo		Balko				Colorado	
	Northwest	North	South	Field	NF	EF	Tower	Pad 1	Pad 2
N	7856	8418	8129	576	803	238	149	720	753
FB_v23132	-0.902	0.314	0.016	-0.297	0.285	-0.157	0.196	0.526	0.723
FB_v22112	-0.890	0.316	0.016	-0.243	0.277	-0.136	0.217	0.604	0.755
RHC_Obs	91.0	130.3	72.6	98.3	217.7	106.3	121.7	196.3	388.9
RHC_v23132	82.9	153.0	129.4	118.8	146.3	138.8	118.7	121.2	180.1
RHC_v22112	64.1	151.4	128.6	105.8	138.4	147.6	104.4	94.1	153.4
RHC_Ratio_v23132	0.911	1.174	1.783	1.209	0.672	1.306	0.975	0.617	0.463
RHC_Ratio_v22112	0.704	1.163	1.773	1.077	0.636	1.389	0.857	0.479	0.394
RHC_FB_v23132	0.093	-0.160	-0.563	-0.189	0.392	-0.266	0.025	0.473	0.734
RHC_FB_v22112	0.347	-0.150	-0.557	-0.074	0.446	-0.326	0.153	0.704	0.868

In summary, comparisons between GRSM23132 and GRSM22112 for all four NO_2 databases, as shown in scatter plots, Q-Q plots, and statistical metrics, indicate that improvements in modeled NO_2 predictions range between a few micrograms to tens of micrograms per cubic meter in favor of GRSM23132 implementation as a Tier 3 screening option. Performance improvements were the most pronounced for the Pala'au and Colorado databases, suggesting the previous GRSM22112 formulation does not adequately account for building effects on enhanced ozone entrainment and downward mixing of NO_X plumes in the cavity and near wake building downwash zones. Improvements from the GRSM23132 treatment of building effects was only slightly indicated for the Balko database, which suggests uncertainties in characterization of building downwash and emissions (for the single dominant short stack) play a role in model-observation comparisons independent of the GRSM23132 treatments. In conclusion, the code updates in GRSM23132 show improved performance over the previous GRSM22112 version, and therefore, the updated GRSM23132 code was implemented in AERMOD version 23132.

A.2 Sensitivity Modeling Results Comparison

Model behavior and sensitivity comparisons between GRSM23132 and GRSM22112 were conducted for five stacks modeled at release heights of 35-meters, 50-meters, and 65-meters with emissions modeled at 1,000 tpy (28.8 g/s) from each stack. The five stacks were positioned north-to-south centered along two adjacent multi-tiered buildings, thus, configured to illustrate differences between GRSM23132 and GRSM22112 treatments of building effected instantaneous ensemble plume dispersion and ground-level concentrations in the near-wake (or building downwash cavity), far-wake (adjacent to the near-wake) zones, and subsequent transition to the near-field distances between 1km and 3km downwind. Figure A.2-1 shows the positioning and multi-tier building complex modeled for the 35-meter, 50-meter, and 65-meter sensitivity scenarios; note the buildings and stacks represent a hypothetical installation and are located and centered at a coastal North Carolina (NC) airport for GRSM sensitivity modeling purposes only. The two adjacent buildings stretch end-to-end 196 meters with varying tier heights. The north building tier heights range 18-29 meters, and the south building tier heights range 11-18 meters. Stack parameters modeled for the 35-meter, 50-meter, and 65-meter scenarios include an exit temperature of 311 K, exit velocity of 7.35 m/s, and stack diameter of 5 meters. BPIPPRM (version 04274) was used to process building tier and stack location data to generate building downwash parameters for input to AERMOD. The building and stack configurations for the three scenarios represent stack height to building height ratios ranging between values of 1.2 and 6.5. This range of stack and building height combinations were included to assess model formulation sensitivities to building downwash and ozone entrainment behaviors under varying meteorological conditions and at varying receptor distances.

Modeled receptors were located and oriented around the stacks and buildings to better identify model formulation sensitivities relevant to the building effects updates in GRSM23132. As such, receptors were positioned at 10-meter spacing surrounding the perimeter of the two buildings at the following distances: 10m, 15m, 20m, 30m, 50m, 75m, 110m, 170m, 250m, and 380m. Fine gridded receptors with 100-meter spacing extending 500m-3km. Medium gridded receptors were modeled with 500-meter spacing extending 3km-15km. Elevations for modeled receptors were based on 1-arc-second USGS terrain data and AERMAP (version 18081) default processing options; receptor elevations indicate relatively flat terrain and are consistent with the coastal study location.

AERMET meteorological inputs to AERMOD were taken from a previous air quality modeling study given it was readily available and that the scope of the GRSM sensitivity focuses on building effects on NO_2 chemistry and dispersion in the near-wake, far-wake, and near field. AERMET (version 19191) raw data inputs included hourly surface temperature, hourly surface wind data, and twice-daily upper air data from a coastal NC airport for a 3-year modeling period 2015-2017. Other AERMET raw data and pre-processing included ASOS 1-minute wind data processed with AERMINUTE (version 15272), 1992 National Landcover Cover Dataset (NLCD) processed with AERSURFACE (version 13016) to generate surface parameters, and AERMET

regulatory default run options.

GRSM NO_2 model input options were configured the same for all scenarios. Hourly ozone for the 2015-2017 modeling period was developed from an isolated rural monitoring station located in Lee County, NC. The AERMOD default ozone value of 0.060 ppm was used for substitution of missing hourly ozone values. Hourly NO_X values were derived from the same Lee County rural monitoring station, and based on an equilibrium ratio of 0.9 NO_2/NO_X, given that only hourly NO_2 data was available; i.e., hourly NO_X values were calculated equal to hourly NO_2 divided by the 0.9 NO_2/NO_X equilibrium ratio. Note the Lee County monitor was located in a farm field greater than 10-20km away from any significant sources of mobile or stationary NO_X emissions sources. Season-diurnal-hourly varying NO_2 concentrations were developed based on the 3-year average, highest-3rd-highest seasonal values from the Lee County hourly NO_2 values 2015-2017. An in-stack NO_2/NO_X emission ratio of 10% was modeled for all five stacks for the three sensitivity modeling scenarios.

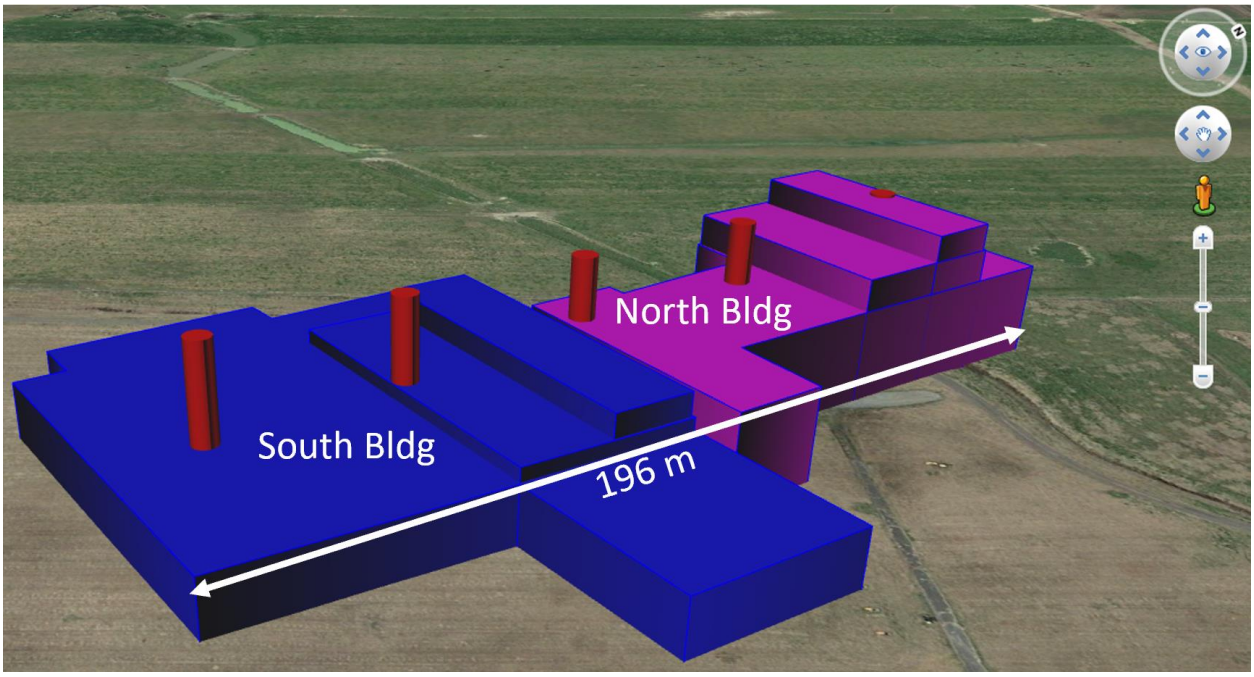

Figure Error! No text of specified style in document.**.2-1 – Sensitivity modeling stack and complex building configuration (graphics shown in Google Earth© and created with Lakes Environmental Software, Inc. AERMOD View©). Note: stacks shown are 30-meters tall.**

Figures A.2-2 through A.2-10 show model concentration contours and difference plots from GRSM23132 and GRSM22112 and for the three sensitivity modeling scenarios. The model results are represented with concentration isopleths derived from the highest-8th-highest 1-hour NO_2 modeled concentrations and correspond with the model design value used in 1-hour NO_2 NAAQS modeling demonstrations (using standard kriging in Surfer version 27.1.229 ®, Golden Software, LLC). Fine and medium gridded receptors are visible as small "+" symbols in each contour plot. Notably, ground level concentrations for the 35-meter stack scenario show

modeled exceedances of the 1-hour NO_2 NAAQS of 188 $\mu g/m^3$ (indicated by a red isopleth) with both GRSM23132 and GRSM22112, whereas modeled concentrations for the 50-meter and 65-meter scenarios show a decrease, relative to the 35-meter scenario, ranging approximately 20%-50% (well below the NAAQS) at all receptors independent of the GRSM code version. Further discussion of model results for each scenario continues below.

GRSM23112 predictions for the 35-meter stack scenario results depicted in Figure A.2-2 range between approximately 10 $\mu g/m^3$ and 200 $\mu g/m^3$ and show approximately 20 $\mu g/m^3$ higher concentrations at receptors located within near-wake zone distances (~10-100 meters) as compared to GRSM22112. Similarly, GRSM22112 maximum concentrations depicted in Figure A.2-3 range between 10 $\mu g/m^3$ and 200 $\mu g/m^3$, but in contrast are roughly 20 $\mu g/m^3$ higher at receptor distances extending from the far-wake (~100-1000 meters) to the near field and out to 1-3km. These differences are spatially isolated and shown in Figure A.2-4 and indicate the GRSM23132 treatment of multiple building effected plumes lowers concentrations in the far wake and near field while enhancing concentrations by equal measure in the near-wake downwash zones. The 35-meter stack scenario stack height to building height ratio values range from 1.2 to 3.5, and thus, NO_X plume size, ozone entrainment, and dispersion is heavily influenced by building downwash as indicated by the maximum concentrations at near and far-wake receptors. And notably, the GRSM23132 building effects treatment for the 35-meter stack and building configuration shows equal sensitivity to modeled concentrations in the near-wake, far-wake, and near field. The 35-meter stack scenario stack and building configuration, and thus, the heavy influence of downwash, is most comparable to the Pala'au, Colorado, and Balko NO_2 evaluation database configurations as well as the distance to near-wake receptor monitor locations. As such, the enhanced concentration model behavior for near-wake receptors shown by the 35-meter stack scenario compliments the improved model performance for similarly configured NO_2 databases while maintaining decreases or no change in modeled concentrations at far-wake and near field receptors.

The 50-meter stack scenario shows less pronounced spatial differences between GRSM code versions than what is shown for the 35-meter stack scenario results at far-wake and near field receptor distances; however, enhanced concentrations at near-wake receptors are relatively more sensitive to GRSM23132 building treatments for the 50-meter stack scenario, albeit at concentrations approximately about 50% lower than those shown for the 35-meter stack scenario. Figure A.2-5 shows the GRSM23132 concentrations are nearly the same as GRSM22112 concentrations shown in Figure A.2-6 in the near field and far-wake downwash zones, and near-wake concentrations modeled with GRSM23132 are enhanced by the building effects treatment formulation. Concentration differences shown in Figure A.2-7 indicate GRSM23132 concentrations for the 50-meter stack scenario are enhanced in the near-wake downwash zone with increases on the order of 50 $\mu g/m^3$. The enhanced concentrations predicted by GRSM23132 in the near-wake zone is complimented by similar enhanced concentrations modeled for several NO_2 model performance databases with similar building effected monitor receptor exposure locations where improved model performance, as previously noted, was shown for Pala'au, Colorado, and some Balko monitors. The sensitivity of the 50-meter stack concentrations to GRSM23132 building effects treatments in the near-wake

zone indicates vertical dispersion becomes relatively more important for taller stacks, or model setup configurations with stack height to building height ratios greater than approximately 1.5; however, this enhanced sensitivity is compensated by lower near-wake concentrations predicted from elevated plume releases and dampened building downwash effects on plume sizes and entrainment of ozone. The converse is observed for stack height to building height ratios below approximately 1.5, where the building effects treatment formulation behavior lowers the sensitivity of increased concentrations in the near-wake while decreasing concentrations due to enhanced lateral dispersion and plume sizes at receptors in the far-wake and near-field.

The 65-meter stack scenario shows model sensitivities similar to the 50-meter stack scenario results, with enhanced concentrations in the near-wake and less differences at far-wake and near-field receptors between GRSM code versions. Again, this is most likely attributed to the more elevated release height of the plume relative to the building height and the GRSM23132 building effects formulation, with the 65-meter stack height to building height ratios ranging between values of approximately 2.1 and 6.5. Figure A.2-8 shows the GRSM23132 concentrations are nearly the same as GRSM22112 concentrations shown in Figure A.2-9 in the near field and far-wake downwash zones, and enhanced GRSM23132 hourly concentrations increasing on the order of 50 $\mu g/m^3$ within the first hundred meters of the near and far-wake. Figure A.2-10 confirms that differences between GRSM23132 and GRSM22112 are relatively unchanged in the far-wake and near field and increased in the near-wake. Near-wake receptor performance improvements indicated by sensitivities shown for the 65-meter stack scenario are less certain than for the 35-meter and 50-meter stack scenarios given that the stack height to building height ratios for all NO_2 databases are closer to values on the order of 1.1 or less, and thus, are not comparable to the 65-meter stack scenario.

In summary, the code refinements evaluated and implemented in GRSM23132 are supported by improved model performance discussed in the previous section and expected code behavior shown by the sensitivity modeling analyses discussed here. GRSM23132 NO_2 predictions show the building effects treatments are less apparent for the taller 50-meter and 65-meter stack scenarios with respect to modeled impacts at receptor distances in the far wake and near field; however, notable enhanced concentrations are shown in the near-wake. The building effects treatments are most pronounced for the 35-meter stack scenario at all receptor distances with lower concentrations modeled at receptors in the far-wake and near field, and equally higher concentrations modeled at receptors in the near-wake building downwash zone. The enhanced higher concentrations modeled for the 35-meter stack scenario at near-wake receptors compliments the improved model performance shown for similarly configured NO_2 databases, and therefore, supports this model behavior. The near-wake behavior of GRSM23132 building effects treatment shows enhanced dispersion and entrainment of ozone that likely contributes to enhanced NO_2 concentrations for shorter stacks and lower stack-to-building height ratios of approximately 1.5 or less. Ultimately, the behavior of the building effects treatment in GRSM23132 is shown to be sensitive to varying model inputs for stack and building heights, improves model performance, and is consistent with the motivation and expected range of predicted NO_2 concentrations at receptors located at distances heavily influenced by building

downwash.

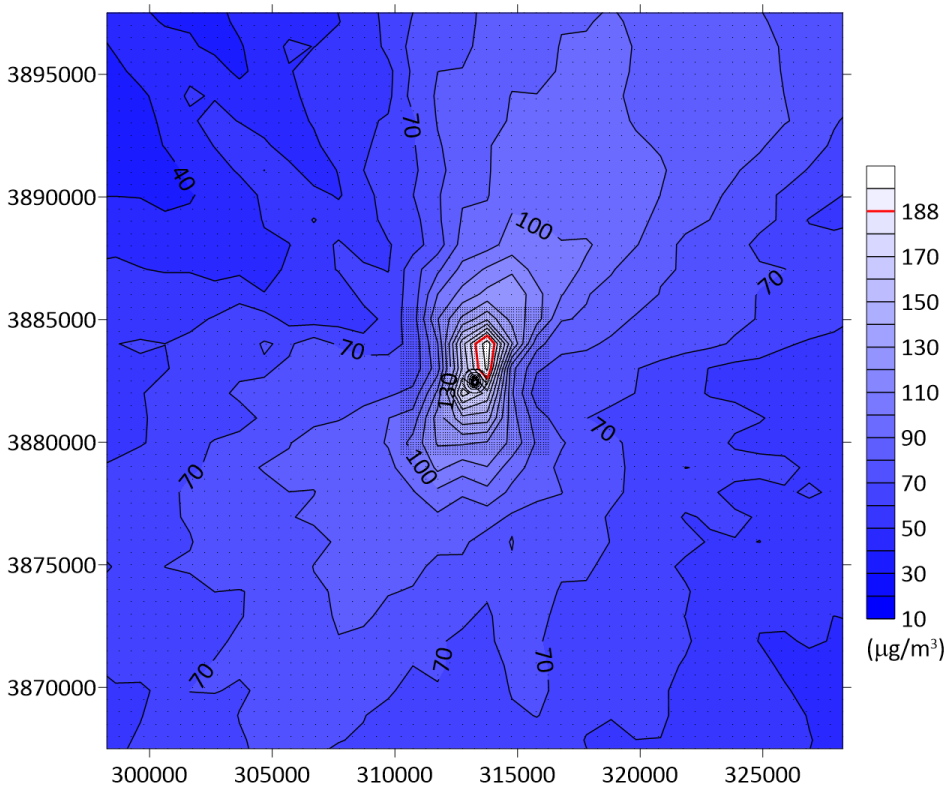

Figure Error! No text of specified style in document.**.2-2 – GRSM v23132 35-meter Tall Stacks Highest-8th-High 1-hour NO_2**

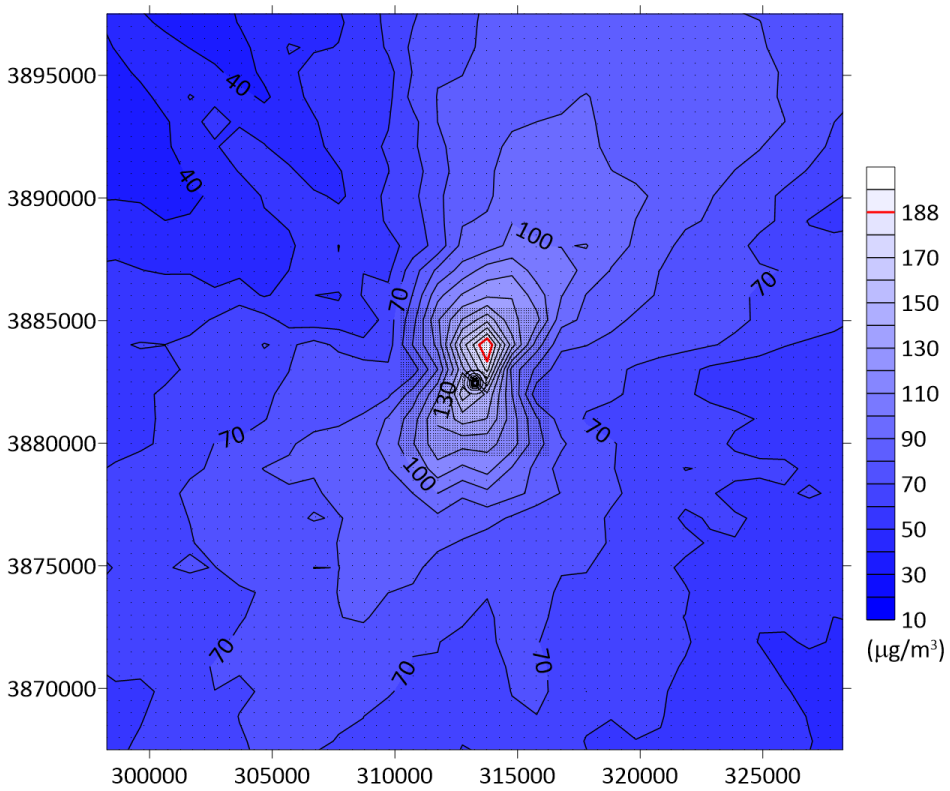

Figure Error! No text of specified style in document.**.2-3 – GRSM v22112 35-meter Tall Stacks Highest-8th-High 1-hour NO_2**

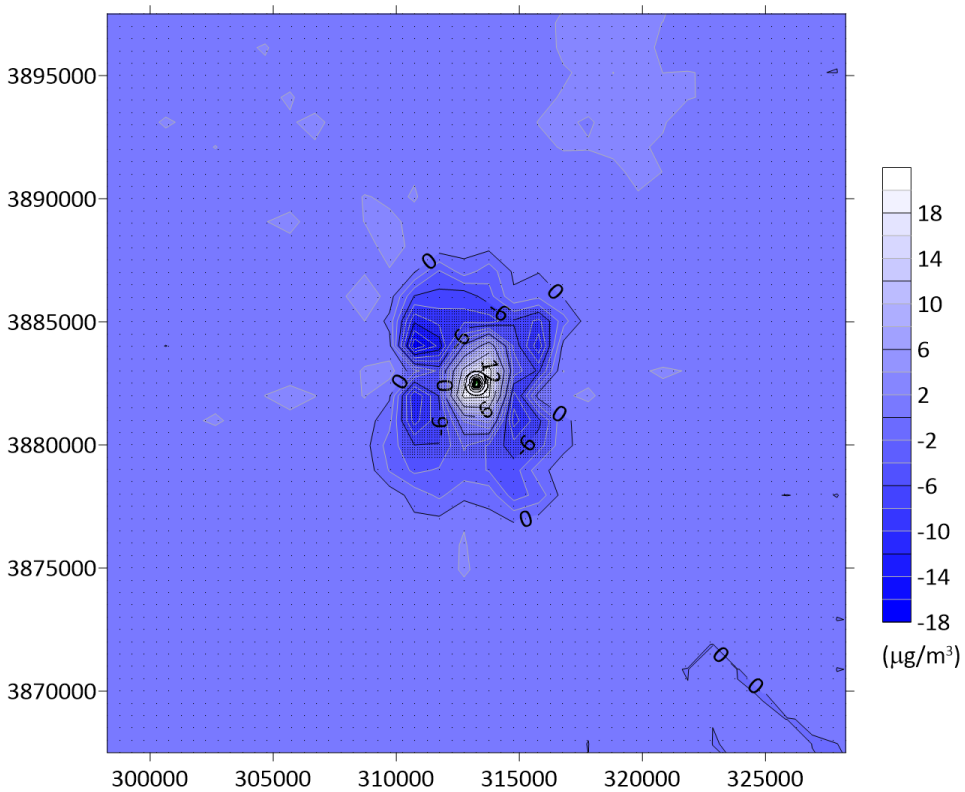

Figure Error! No text of specified style in document.**.2-4 – GRSM v23132 Minus v22112 35-meter Tall Stacks Highest-8th-High 1-hour NO_2**

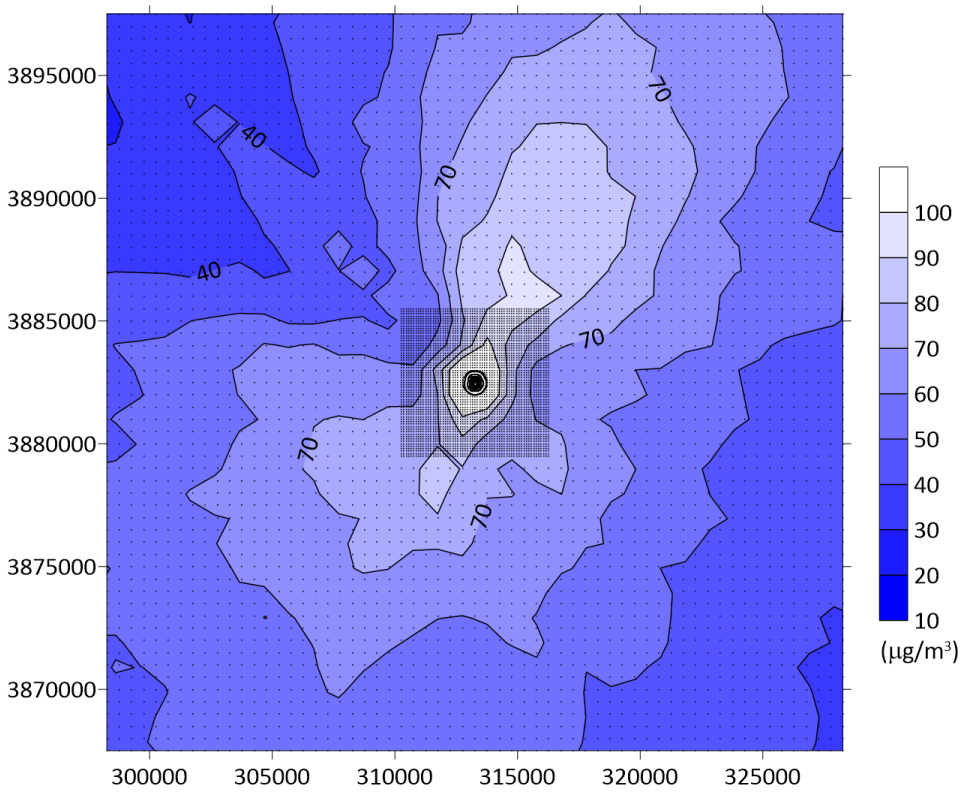

Figure Error! No text of specified style in document.**.2-5 – GRSM v23132 50-meter Tall Stacks Highest-8th-High 1-hour NO_2**

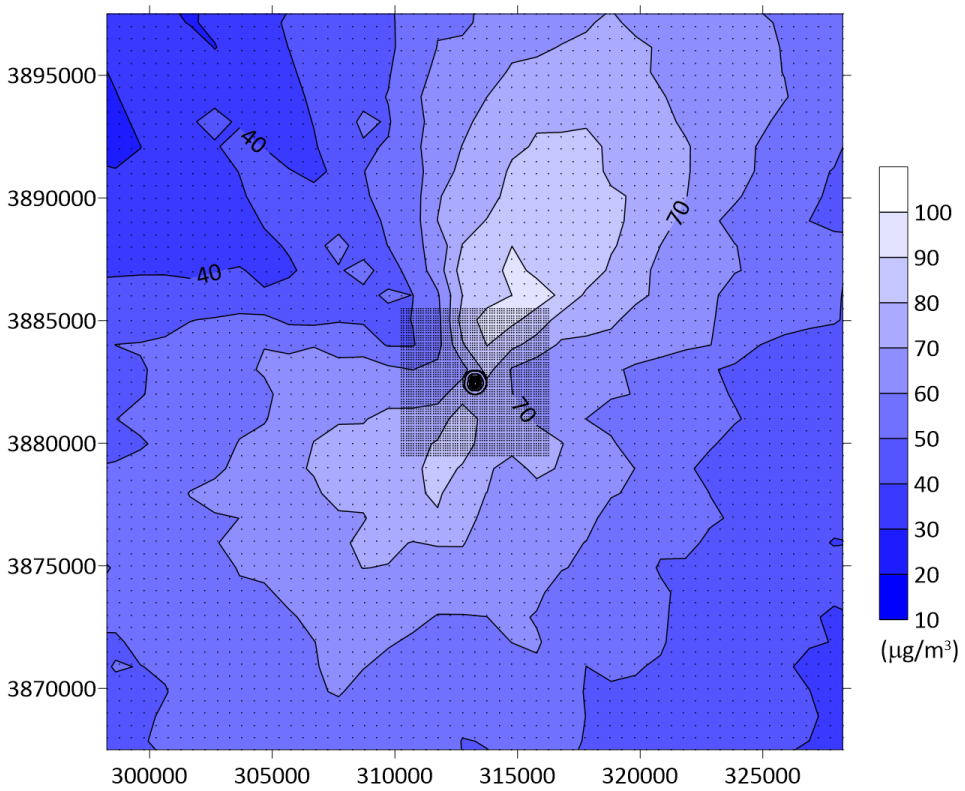

Figure Error! No text of specified style in document.**.2-6 – GRSM v22112 50-meter Tall Stacks Highest-8th-High 1-hour NO_2**

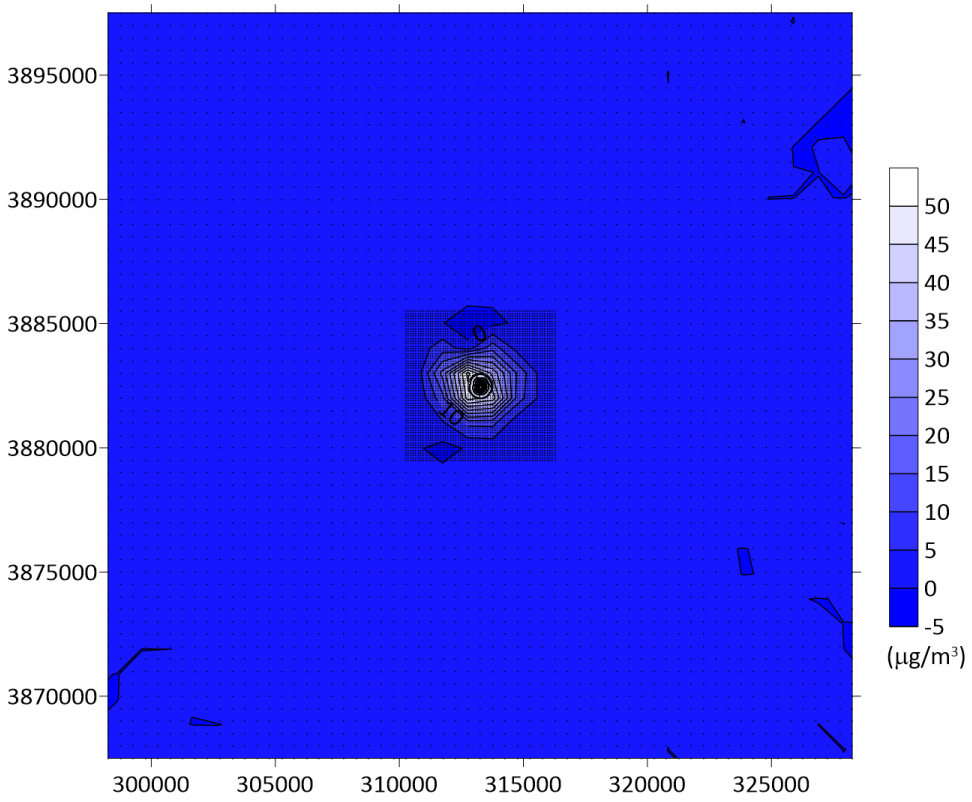

Figure Error! No text of specified style in document..**2-7 – GRSM v23132 Minus v22112 50-meter Tall Stacks Highest-8th-High 1-hour NO_2**

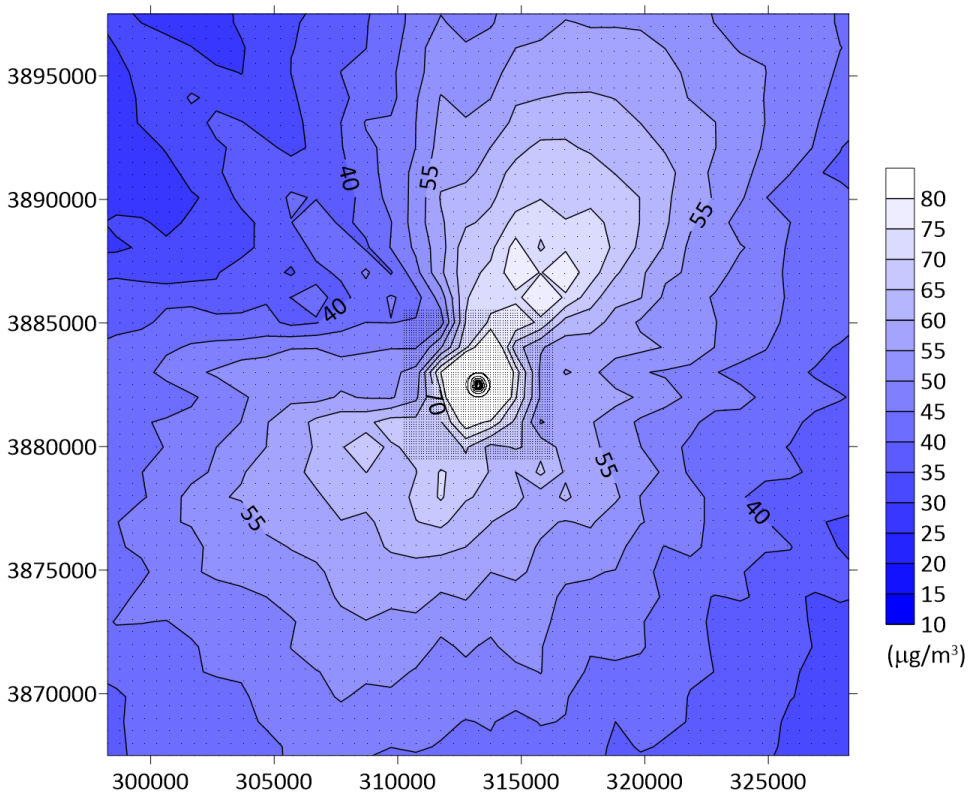

Figure Error! No text of specified style in document..**2-8 – GRSM v23132 65-meter Tall Stacks Highest-8th-High 1-hour NO_2**

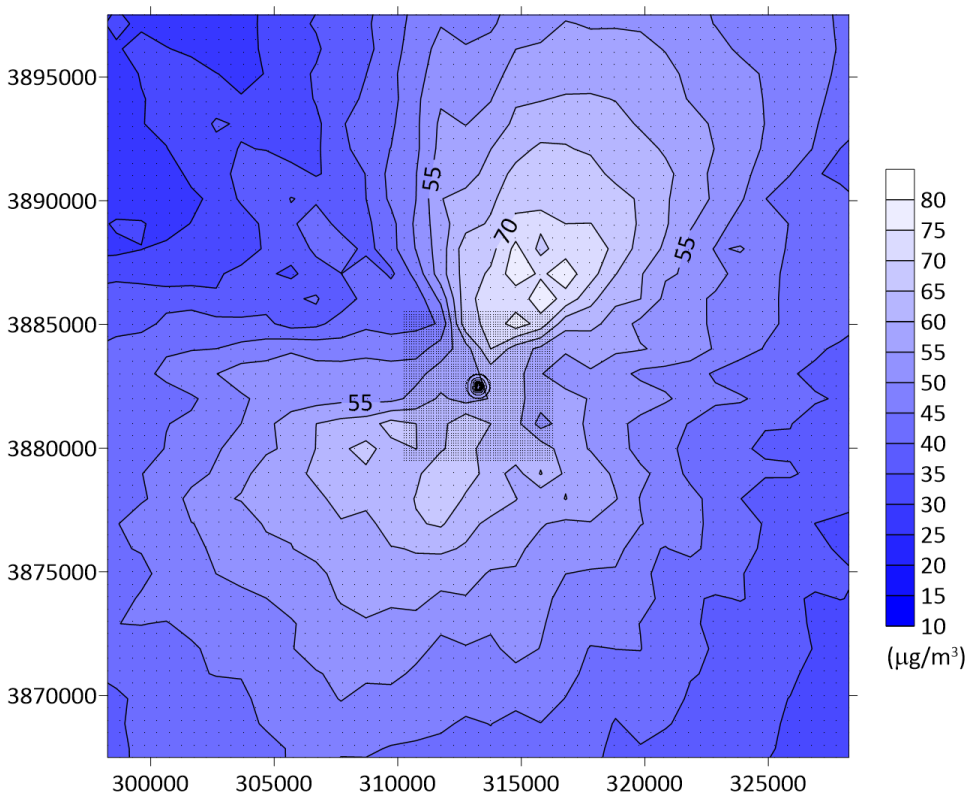

Figure Error! No text of specified style in document.**.2-9 – GRSM v22112 65-meter Tall Stacks Highest-8th-High 1-hour NO_2**

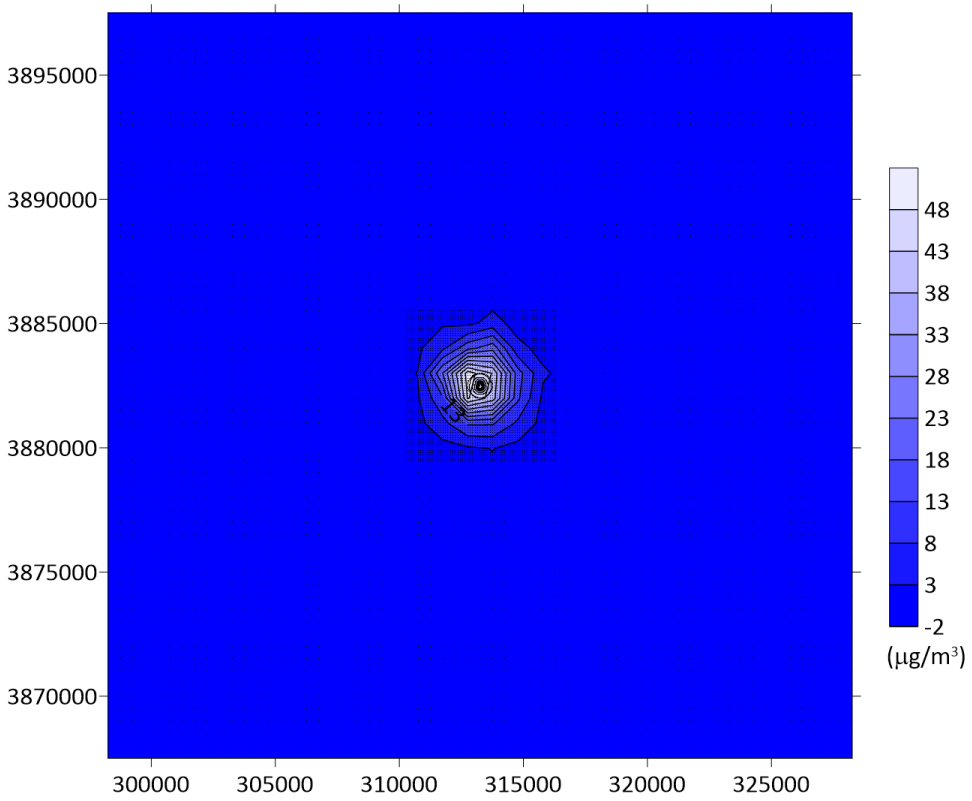

Figure Error! No text of specified style in document.**.2-10 – GRSM v23132 Minus v22112 65-meter Tall Stacks Highest-8th-High 1-hour NO_2**

United States Environmental Protection Agency	Office of Air Quality Planning and Standards Air Quality Assessment Division Research Triangle Park, NC	Publication No. EPA-454/R-24-005 November 2024